New Approach to Drug Product Process Design:
Leveraging First Principles Modeling and Cross-Product Process Monitoring to Improve Process Design Robustness

by

Nahathai Srivali

B.S. Chemical Engineering, Massachusetts Institute of Technology, 2010

Submitted to the MIT Sloan School of Management and the Department of Mechanical Engineering in Partial Fulfillment of the Requirements for the Degrees of

Master of Business Administration
and
Master of Science in Engineering Systems

In conjunction with the Leaders for Global Operations Program at the Massachusetts Institute of Technology

June 2015

Signature of Author Signature redacted
MIT Sloan School of Management, MIT Department of Engineering Systems
May 8, 2015

Certified by Signature redacted
Arnold Barnett, Thesis Supervisor
Professor of Management Science, MIT Sloan School of Management

Certified by Signature redacted
Anthony Sinskey, Thesis Supervisor
Professor of Biology and Engineering Systems

Accepted by Signature redacted
Munther A. Dahleh
William A. Coolidge Professor of Electrical Engineering and Computer Science
Chair, ESD Education Committee

Accepted by Signature redacted
Maura Herson, Director of MIT Sloan MBA Program
MIT Sloan School of Management

This page intentionally left blank.

New Approach to Drug Product Process Design:
Leveraging First Principles Modeling and Cross-Product Process Monitoring to Improve Process Design Robustness

by

Nahathai Srivali

Submitted to the MIT Sloan School of Management and the MIT Department of Engineering Systems on May 8, 2015 in Partial Fulfillment of the Requirements for the Degrees of Master of Business Administration and Master of Science in Engineering Systems

Abstract

The vision of the Operations Technology Group at Amgen is to enable a robust pipeline through focused and efficient operations research studies. Process design is traditionally developed by performing experiments, but other approaches can be used to improve cost, efficiency, and robustness. The scope of this internship included the use of First Principles, Computational Fluid Dynamics (CFD), and Cross-Product Process Monitoring (CPPM) to improve process design robustness with reduced testing and faster development cycle. The project focused specifically on the drug product development network, which included the development of processes from formulation to filling and finishing, clinical manufacturing, and technology transfer to commercial manufacturing

The goal of this internship was to explore opportunities to utilize First Principles, CFD, and CPPM in drug product process design space. First Principles and CFD modeling tools were used to look into the physics of drug product filling process (specifically parameters influencing two key filling issues – drying during line stoppage and dripping between fills). Criteria for analyzing cost and benefits for the use of First Principles were also provided as strategic recommendations on where the new approach should be utilized.

Clinical data were leveraged, with multivariate statistical data analysis, to determine inspection reject limit for the purpose of process monitoring and root cause analysis.

Thesis Supervisor: Arnold Barnett
Title: George Eastman Professor of Management Science, Professor of Statistics

Thesis Supervisor: Anthony Sinskey
Title: Professor of Biology and Engineering Systems

This page intentionally left blank.

Acknowledgments

I would like to give my sincerest thanks to the Leaders for Global Operations program and everyone at Amgen who supported me in the completion of this thesis.

I learned tremendously from my advisors, Arnie Barnett and Tony Sinskey, and my Amgen mentors, Wenchang Ji, Adrian Distler, and Matthew Kasenga. Their knowledge, passion, and guidance were both inspiring and invaluable to the success of the internship.

Viraj Kamat and Suresh Nulu, you were crucial in the successful completion of my work at Amgen. Thank you for being experts in your fields and transferring the knowledge to me. More importantly, I appreciate your friendship and motivation.

I was particularly impressed by the leadership team behind the Amgen-LGO partnership - Sam Guhan, Bill Rich, Dave Stadolnik, Leigh Hunnicutt, and Eric Dolak. I cannot imagine a better internship experience elsewhere. The industry experience, work scope, and intern activities were truly designed with the interns in mind. Aspan Dahmubed, Nick Hasara, and Daniel Lee, thank you for your guidance. I also appreciated the support of my LGO network at Amgen – Spencer Anderson, Cathy Fang, Steve Fuller, Amy Lee, Nick Sazdanoff, Seth White, Marie Wolbert, and , Maxine Yang.

Wendy Chen, Javi Hernandez, Garnet Kim, Willow Primack, and Ann Weeks, you guys were part of the highlights of my time in Southern California. Thank you for welcoming me warmly and making me feel amazing during the time away from home.

Lastly, I thank my family. They made me who I am today, and I owe everything to them. My parents, Vuthikorn and Patcharee Srivali, are the most devoted parents and best friends a daughter can ask for. My brother, Dr. Narat Srivali of Mayo Clinic, is my inspiration. Uncles Eak, Aoy and Tum as well as Aunt Tuk, without you guys, I would not have made it to MIT for my Bachelor's degree, let alone my two Master's.

This page intentionally left blank.

Table of Contents

List of Figures

List of Tables

List of Equations

This page intentionally left blank.

1 Background and Introduction

1.1 Biotechnology

1.1.1 Industry Background

The biotechnology industry consists of companies that develop, manufacture, distribute, and/or sells biologics. Biologics are drugs derived from living organisms, as opposed to chemical compounds that make up traditional pharmaceutical drugs. They are designed to target specific cells associated with various medical conditions. In contrast to most drugs that are chemically synthesized and whose structures are known, biologics are complex mixtures that are not easily identified or characterized. They include therapeutic proteins, DNA vaccines, monoclonal antibodies, as well as gene therapy.

The biotechnology industry first emerged in the 1970s with the development of recombinant DNA technology, enabling the transformation of DNA sequences into protein-based drugs that resemble natural substances. The first non-vaccine biologic was biosynthetic insulin developed by Genentech and introduced in 1982. Since then, the industry has experienced incredible growth attributable to new product development, a favorable regulatory environment, an aging population, and increased access to capital. The future of the industry will likely be shaped by a combination of factors, including the entry of biosimilars after patent expiry, increasing mergers, acquisitions and consolidation among the players, trends in drug pricing and reimbursement policy requiring lower prices, impact of demand for personalized medicine, and changing disease trends (JP Morgan, 2015).

The development of a biologic typically takes over 10 years from discovery to market. Furthermore, only a fraction of these developments reach the market. It is estimated that 90% of the money spent researching new treatments is spent on failures, meaning that biotechnology companies spend as much as $2 billion for each successful drug. Companies must rely on the revenues from the drugs that are successful to cover the costs associated with research and development. Competition within the biotechnology industry is very high with a strong focus on first-mover advantage (IBIS World, 2015).

1.1.2 Biotechnology Process Overview

Manufacturing biologics is a complex process with strict process controls, long lead times, and high fixed costs of operations. The process involves the following four major steps: 1) master cell line generation; 2) cell growth and protein production; 3) protein isolation and purification; and 4) product preparation for humans.

The cell line production begins with specifications of manufacturing methods and the drug's physical form (e.g., infusion or injection) modified for large-scale production to meet product demands. A cell line is selected, typically from deriving Chinese hamster ovary (CHO) or *E. coli* cell lines. Once selected, the cell line is cryopreserved, the process by which a large quantity of vials containing the desired cells are frozen to create a cell bank. Cell banks include a master cell bank (MCB) and a working cell bank (WCB). The MCB is used only when absolutely necessary, while the WCB is used to produce products.

During the upstream production, the cells from the WCB are grown in a flask containing growth media. The cell culture is then scaled-up by being transferred into larger and larger growth vessels and more fresh growth media to facilitate cell growth and production. Cell viability, concentration, and various environmental conditions are constantly monitored for quality purposes.

In the downstream phase, protein is isolated from the cell culture and purified. The cells are broken apart to isolate protein product, which is then run through a series of chromatography and filtration steps for purification. The product is then diluted to the desired concentration, resulting in drug substance (DS) or drug substance intermediate (DSI) contained in either carboys or cryovessels.

Finally, the product passes through the formulation, fill, and finish (FFF) stages during which the DS is formulated and presented per specifications for patient use in a final presentation form, such as a vial or pre-filled syringe. These processes translate the DS to Drug Product (DP). The FFF process includes formulation and mixing, bioburden filtration, and then an in-process hold before going through sterile filtration, product filling, and lyophilization (for some products). Finally, the DP is inspected, labeled, packaged, and shipped (Meyer, 2012).

1.2 Amgen

Amgen, Inc. was founded in 1980 with the mission "to serve patients." Since then, Amgen has grown to become the world's largest independent biotechnology company with approximately 20,000 employees, total revenue of $18.7 billion, product sales of $18.2 billion, and R&D expenses of about $3.9 billion for the year

2013. The company focuses solely on human therapeutics with the following 13 products in the market: Aranesp®, BLINCYTO™, Enbrel®, EPOGEN®, Kyprolis®, Neulasta®, NEUPOGEN®, NEXAVAR®, Nplate®, Prolia®, Sensipar®/ Mimpara®, Vectibix®, and XGEVA® (Amgen, Inc., 2015). To facilitate the production of these products, Amgen has facilities in California, Kentucky, Puerto Rico, Rhode Island, Ireland and the Netherlands. Additionally, Amgen broke ground on an innovative manufacturing facility in Singapore in 2013.

While Amgen continues to grow and increase sales year after year, a few major challenges lie in the years ahead. First, several of its blockbuster drugs are nearing the end of their patent life. Secondly, as more and more companies improve their drug discovery capabilities, competition to be the first to bring a new drug to market has increased. Both of these challenges have pushed Amgen to actively expand its product pipeline. As of February 2014, Amgen has 20 products in Phase 1, 10 products in Phase 2, and 16 products in Phase 3 (Amgen, Inc., 2014). Amgen has undertaking a number of cost-cutting measures as a way to improve operational efficiency and to ensure the company's long-term financial and operational well-being.

1.2.1 Drug Product Commercialization and Manufacturing Network

The work presented in this thesis is part of Amgen Drug Product Commercialization and Manufacturing Network, which focuses on the development, commercialization, and manufacturing of Drug Product (DP).

Before the drug product can be manufactured for the clinical or commercial scale, process design - the development by which appropriate drug product formulation as well as appropriate process parameters for each unit operation are defined – needs to be completed and tested at the lab scale. The process is then followed by technology transfer – the procedure by which parameters determined during process design are introduced to the clinical and commercial environments to ensure consistencies across scales and equipment differences. DP process design and technology transfer involve four major functional groups comprising Amgen's Drug Product Commercialization and Manufacturing Network. These groups are Drug Product Development (DPD), Drug Product Technology (DPT), Clinical Manufacturing, and Commercial Manufacturing (Figure 1).

Figure 1: Amgen's Drug Product Commercialization and Manufacturing Network

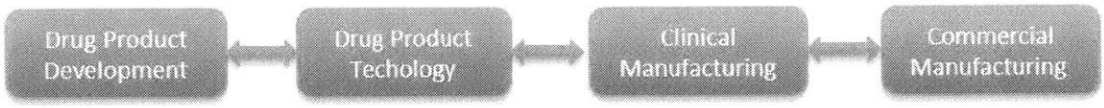

A major goal of the network is to achieve better alignment across the groups that encompass it and to approach the work together as a network. This goal is particularly important as Amgen is expanding its product profile as well as manufacturing sites, each of which has different requirements and equipment. Accomplishing this will enable Amgen to improve operational efficiency and speed up process design and technology transfer process.

The manufacturing process of DP was discussed in the Biotechnology Process Overview section earlier and is summarized in the figure below.

Figure 2: Drug Product Manufacturing Process

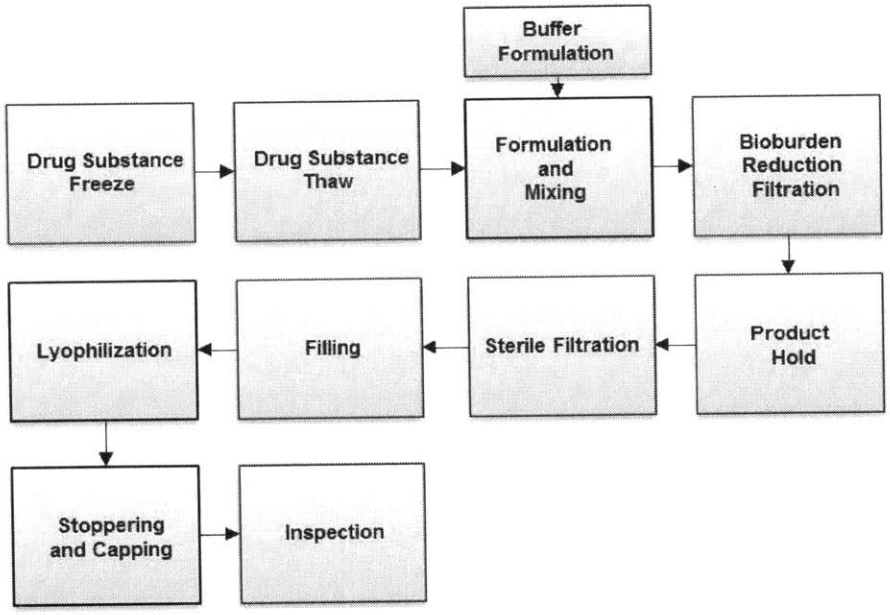

1.2.2 The Drug Product Technology Group

This project focuses on the DPT group and its crucial connections across the Drug Product Network. DPT comprises of several smaller groups that develop processes and support manufacturing. Once DPD recommends a formulation that is stable and robust, DPT performs studies to assess drug product manufacturability and recommends specific equipment settings and critical process parameters ranges to clinical and commercial manufacturing. DPT plays a critical role from providing data for regulatory filing to supporting manufacturing through technology transfer and non-conformance investigations.

1.3 Project Introduction

1.3.1 Problem Statement

Traditionally, process design is developed by performing experiments, but such an approach can often be resource intensive and generates limited view of the parameters' impact on a given process. Other approaches can improve efficiency and robustness of process design by providing holistic understanding of how process variables interact. Ultimately, the goal is to better design target experiments and speed up process development, while sustaining the quality of the product.

Such new approaches include leveraging First Principles, Computational Fluid Dynamics (CFD) modeling, and feedback from clinical and commercial manufacturing through process monitoring.

1.3.2 Project Approach

To illustrate feasibility and benefits of the above approaches to process design, three targeted case studies in filling unit operation were utilized. In the first case study, First Principles were used to determine the maximum stoppage time before a filling nozzle becomes clogged with dry drug product, causing disruption in the filling process. In the second case study, Computational Fluid Dynamics (CFD) was used to help visualize and understand the impact of operating parameters on filling process performance (as shown by splashing and dripping phenomena). In the third case study, data generated at a clinical scale through process monitoring were leveraged to illustrate improvement opportunities and highlight risks.

2 Case Studies

2.1 Utilizing First Principles to Predict Maximum Stoppage Time before Drying Becomes a Problem in Filling Unit Operations

2.1.1 Project Summary

Drug product drying at the filling nozzle is a problem during process development and manufacturing and can cause filling disruptions and scrap. The previous method of estimating the maximum disruption-caused stoppage time for a filling line was through direct experiments on the manufacturing line, which required extensive line time and resources. The experiments were typically run in the later phases of process development, which limited the ability to provide timely feedback for designing the process. This project sought to gain information about drying earlier in process development and thereby to reduce manufacturing line time.

To achieve this goal, the Ranz-Marshall mass transfer correlation was used to identify key First Principles parameters that affect the rate at which the drug product dries at the filling nozzle during extended stoppage times of the filling. A First principles model seeks to calculate physical quantities based directly on established laws of physics, without making assumptions or relying on empirical or fitted parameters. Starting at the foundations, First Principles modeling allows us to not miss any important parameters that were not thought of when designing experiments. From the model, the key parameters were identified as: filling room relative humidity, air temperature, air flow, product temperature, inner diameter of

nozzle used to fill the product, and change in product concentration from the beginning to the end of stoppage time.

Because the product concentration at the end of stoppage time is required to estimate a key parameter, experiments had to be performed to see how the product concentration changes over time (whether it is linear, for example). The experiments also could help confirm whether the drying rates estimated from the First Principles model were comparable to those arising in real experiments , in which case the model could be used subsequently to limit or eliminate the experiments. The First Principles model and the experimental results complemented one another: the model called attention to variables that were important in understanding the drying process but was not precise in explaining how these variables affect the drying time across manufacturing conditions. A quantitative formulation, such as Design of Experiments (DOE), can "flesh out" the insights that the First Principles model brought forth.

Using the parameters found in the First Principles model, a DOE that covered all the key parameters was created to target laboratory experiments and produce a customized model for the drying process under study. A tensiometer, an instrument that measures surface tension of a liquid, was used. It employs the pendant drop method to capture surface tension as well as drug product droplet volume over time, allowing us to capture how protein concentration changes over time under different concentrations. As the First Principles model made clear, estimating these changes was important in describing the drying process.

Two key findings arose from the experiments. The first deals with the change in protein concentration over time. The tensiometer experiments showed that the change in protein concentration is not linear over time. There is a quick drop in the surface tension and thus an increase protein concentration early in the process before the droplet stabilizes. After a period of stabilization, there is a second rapid drop in surface tension as the droplet transitions into a viscoelastic gel; this phase ends as the droplet becomes a stable gel and the surface tension and droplet volume do not change further in this regime. Each drug product has a unique critical concentration at which it dries to the point of filling line disruption. That critical concentration is the concentration of drug product, just before the second rapid drop in surface tension as the droplet transitions into a viscoelastic gel. Because of the unique critical concentration, the First Principles model in itself cannot predict the drying time for a drug product. However, the First Principles can be used to understand the drying rate, or how fast the drug product evaporates to that critical concentration. The second key finding from the experiments was that the Ranz-Marshall mass transfer correlation was able to predict the drying rates similar to those of the experiments.

From these two discoveries, we were able to recommend that 1) a set of tensiometer experiments be performed for each drug product to acquire the unique critical centration of the drug product and 2) Ranz-Marshall mass transfer correlation be used to identify the rate at which the concentration gets to the critical point. This knowledge can help avoid the filling line disruption by providing the early feedback to design, allowing researchers to find a different manufacturing

condition with key parameters that optimize the maximum disruption-caused stoppage time for a filling line.

The understanding of critical concentration and drying rate helps us understand the impact of various parameters (e.g., humidity, product temperature, product attributes, and nozzle size) on drug product drying times at the filling nozzle, allows for a more holistic understanding of the problem, and provides insights into important considerations for the technology transfer. This understanding provides an opportunity to investigate changes in key parameters, extend the time it takes before the second rapid drop in surface tension happens and reduce the chance of filling line disruption during manufacturing.

2.1.2 Project Introduction

2.1.2.1 Motivation

Transferring drug product from a large container to small vials or syringes during the filling process, there can be disruptions. During these interruptions over time, the liquid drug product at the end of the filling nozzle can evaporate. Depending on the length of line stoppage time, the evaporation can cause problems such as splashing when the line starts back up again. This causes product rejects due to improper drug concentrations.

The maximum stoppage time before a drug product is dry to the point where disruption becomes a problem varies by product and operating environmental conditions. The existing method of evaluating the maximum stoppage time is through integrated line studies, where process development engineers shut clinical

and commercial manufacturing lines down to perform the study. Such study setup is expensive, inefficient and only evaluates one set of environmental conditions at a time.

2.1.2.2 Project Approach

First Principles can be used to describe the mass transfer that happens during extended stoppage times of the filling line when the drug product dries at the filling nozzle. This research utilized the First Principles to create a predictive model for maximum stoppage time across different parameter conditions.

To evaluate the results from the First Principles predictive model, an experimental setup with a tensiometer was utilized. A tensiometer is an instrument that measures surface tension of a liquid. One type of tensiometer uses the pendant drop method to capture surface tension as well as drug product droplet volume over time. The theory behind the pendant drop method will be discussed in the next section. The results of the First Principles predictive model were compared with those from the tensiometer experiments. Additionally, a few sets of filling experiments were completed to mimic integrated line studies and confirm the results from stoppage time studies.

The First Principles predictive model and tensiometer studies have advantages over the traditional integrated line studies for a number of reasons. The tensiometer measurements can be done in the lab environment and is thus more cost-effective than the integrated line study, increase flexibility to conduct study unrestricted by plant availability, and highlight products with drying risk before technology transfer. The model can be used to understand the impact of various

parameters (e.g., humidity, product temperature, product attributes, and nozzle size) on drug product drying times at the filling nozzle, allowing for a more holistic understanding of the problem and providing insights into important considerations for the technology transfer. The overall purpose of the study is to evaluate the use of tensiometer studies for determining critical concentration of drug product at which nozzle becomes clogged and of First Principles predictive model for determining the rate at which the drug product dries.

2.1.3 Background Information

2.1.3.1 Mass Transfer Correlation for Evaluating Parameters Affecting Drying

Drug product drying at the end of a filling nozzle can be modeled in a mass transfer problem as a droplet at the end of tubing. For mass transfer from a spherical droplet subjected to the relative velocity of a drying medium (such as air), Ranz-Marshall mass transfer correlation can be used (Wilkes, 2005).

Equation 1: Ranz-Marshall Equation to Find Mass Transfer Coefficient

$$Sh = 2 + 0.6Re^{0.5}Sc^{0.33}$$

Sherwood number (Sh) is a dimensionless number representing the ratio of convective to diffusive mass transport. It is defined, as follows:

Equation 2: Definition of Sherwood Number

$$Sh = \frac{K * L}{D} = \frac{Convective\ mass\ transfer\ coefficient}{Diffusive\ mass\ transfer\ coefficient}$$

where

- L is a characteristic length (m), which is the diameter of the nozzle in this case
- D is mass diffusivity (m^2/s) for vapor in the air (related to air temperature)
- K is the mass transfer coefficient (m/s)

Reynolds number (Re) is a dimensionless number used to help predict similar flow patterns in different fluid flow situations. It is defined as the ratio of inertial forces to viscous forces and consequently quantifies the relative importance of these two types of forces for a given flow condition.

Equation 3: Definition of Reynolds Number

$$Re = \frac{\rho \vartheta L}{\mu}$$

where

- μ is dynamic viscosity of drug product (kg/m-s)
- ϑ is velocity of air flow (m/s)
- ρ is product density (kg/m^3)

Schmidt number (Sc) is a dimensionless number to characterize fluid flows where there are simultaneous momentum and mass diffusion convection processes.

Equation 4: Definition of Schmidt Number

$$Sc = \frac{\vartheta}{D}$$

From the Ranz-Marshall equation, the mass transfer coefficient (K, m/s) can be obtained. K is then used to determine the evaporation rate (R) at which the drug product dries:

Equation 5: Evaporation Rate

$$R = KA_p\, M_p(C_s - C_g)$$

where

- A_p is the surface area of the droplet (m^2)
- M is the molar mass of the droplet (g/kmol)
- C_s is the vapor concentration at the droplet surface ($kmol/m^3$) and defined as follows:

Equation 6: Vapor Concentration at Droplet Surface

$$C_s = \frac{p_{sat}(T_p)}{RT_p}$$

- C_g is the vapor concentration in the bulk air ($kmol/m^3$) and defined as follows:

Equation 7: Vapor Concentration at Bulk Gas

$$C_g = X_i \frac{p_{op}}{RT_g}$$

Given the parameters found in the First Principles mass transfer model, variables that affect the drug product drying rate were identified. They are shown below in Table 1:

Table 1: Variables in First Principles Model

Category	Parameter
Filling room environment	Relative humidity
Filling room environment	Air temperature
Filling room environment	Air flow
Filling condition	Product temperature
Filling condition	Nozzle ID
Product	Product concentration at start of production

2.1.3.2 Pendant Drop Measurements from the Tensiometer Study

Surface tension measurements through pendant drop method utilize the theory that a stationary pendant drop has only two forces acting on it: gravity and surface tension (Woodward, 2014).

The Young-LaPlace equation gives the pressure difference across the drop interface (First Ten Angstroms, 2000):

Equation 8: Young-LaPlace Equation

$$\Delta P = \gamma(\frac{1}{R_1} + \frac{1}{R_2})$$

Where

- ΔP is the pressure difference across the interface
- γ is surface tension of the liquid
- R_1, R_2 are radii of curvature

As for the gravitation force, pressure drop for a liquid drop is as follows:

Equation 9: Pressure Drop in Liquid

$$\Delta P = \rho g h$$

Where

- ρ is the density of the liquid
- h is the height of the droplet under the influence
- g is the acceleration due to gravity

The tensiometer with pendant drop method works by solving Equation 8 and Equation 9 to get the surface tension of the liquid droplet.

2.1.4 Materials and Methods

The materials and equipment utilized for the tensiometer and filling studies are specified in the following tables.

Table 2: List of Materials and Equipment Common for Both Tensiometer and Filling Studies

Component/ Equipment	Equipment Number
Drug Product A at 70 mg/mL	Amgen, Inc. (1:1 Dilution of 140mg/mL)
Drug Product A at 140 mg/mL	Amgen, Inc.
Drug Product A Buffer	Amgen, Inc.
1.0mm Filling Nozzle	Flexicon 30-030-010
2.5mm Filling Nozzle	Flexicon 30-030-020

Table 3: List of Materials and Equipment for the Tensiometer study

Component/ Equipment	Equipment Number
Pendant Drop Tensiometer	FTA1000
Fan	Orion Fans CA109AP-11-1 TB
Vacuum Pump	Barnant Co. 400-1941
Humidity Meter	Eletrotec 968366
Dehumidifier Controller	ETS Microcontroller 5100
Flow Meter	Alltech 820 Mass Flowmeter
Filling Noozles	NORM-JECT® Luer
30G Needle	SAI B30-50
Software	FTA32
High-Speed Video Camera	Olympus iSpeed TR
JMP Statistical Software	JMP version 11

Table 4: List of Materials and Equipment for the Filling Study

Component/ Equipment	Equipment Number
250 mL Surge vessel	KIMAX
3/8" Tubing	Accusil
1.2mm Tubing	Accusil 84-103-012
0.8mm Tubing	Accusil 84-103-008
Y Connector	Accusil 84-012-002
Peristaltic Pump	Flexicon 61-150-022
High- Speed Video Camera	Olympus iSpeed TR

2.1.4.1 Design of Experiments

Ranges of variables affecting drug product drying rate were identified using ranges of manufacturing conditions across products and sites. They are shown below in Table 5.

Table 5: Ranges of Conditions Studied

Category	Parameter	Range Studied
Filling room environment	Relative humidity	30%, 60%
Filling room environment	Air flow	0, 0.5 m/s from the top
Filling condition	Product temperature	5ºC, 20ºC
Filling condition	Nozzle inner diameter	1mm, 2.5mm
Product	Product concentration	70mg/ml, 140mg/ml

From these ranges, a fractional factorial experimental design was developed to evaluate the First Principles model and the tensiometer study. Table 6 shows the Experimental Design:

Table 6: Experimental Design for the Study

Experiment Number	Relative Humidity (%)	Air Flow from the Top (m/s)	Product Temperature (°C)	Nozzle ID (mm)	Concentration (mg/ml)
1	30	0	5	1	70
2	60	0.5	5	1	70
3	60	0.5	20	1	70
4	30	0	5	1	140
5	60	0	20	1	140
6	60	0.5	20	1	140
7	30	0.5	20	2.5	70
8	60	0	5	2.5	70
9	60	0	20	2.5	70
10	30	0.5	5	2.5	140
11	30	0	20	2.5	140
12	60	0.5	5	2.5	140

2.1.4.2 Experiment Setup

2.1.4.2.1 Surface Tension and Drying Time Measurements

Pendant drop readings were taken per the Amgen's standard operating procedure. 2.5 mL of sample was drawn using a 3 mL syringe. The syringe was fitted with a filling nozzle and placed into the holder. The filling nozzle was connected to the syringe via tubing. A pendant shape was manually formed on the needle tip, and images were acquired every 10 seconds for a 2 hour period. Initial drop volumes were highly dependent on the nozzle size used. Images were

analyzed to yield surface tension results using the surface tension estimator software, which came with the pendant drop tensiometer equipment, called FTA1000. Figure 3 shows the experimental setup and representative image of the droplet.

Figure 3: Pendant Drop Instrument Setup and Representative Image

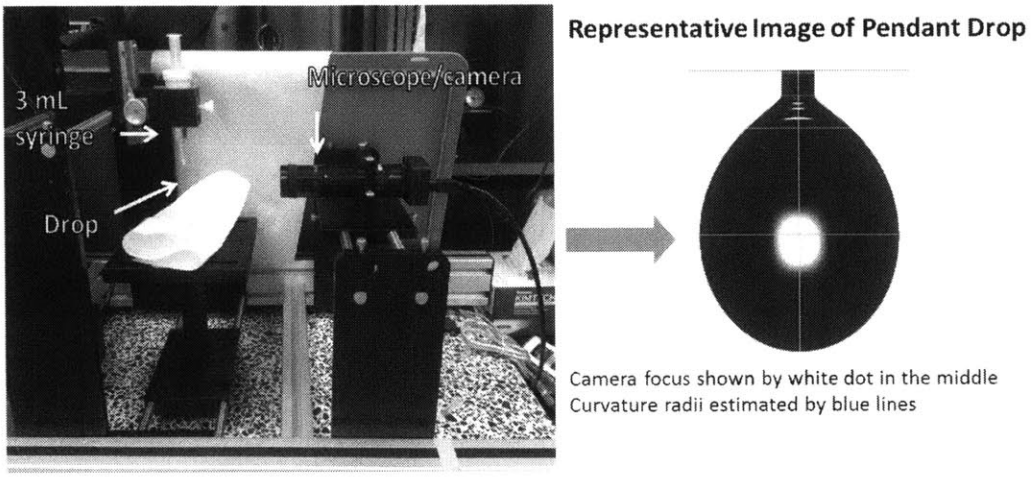

To lower the humidity of the setup, the tensiometer was covered with a transparent plastic bag to create a sealed chamber (as shown in Figure 4 below). Moist air was sucked out of the chamber by a vacuum pump, passed through a desiccator column, and circulated back into the chamber. The pump was controlled by a feedback control unit that was connected to a humidity probe in the chamber.

Figure 4: Experimental Setup for Controlled Humidity Environment

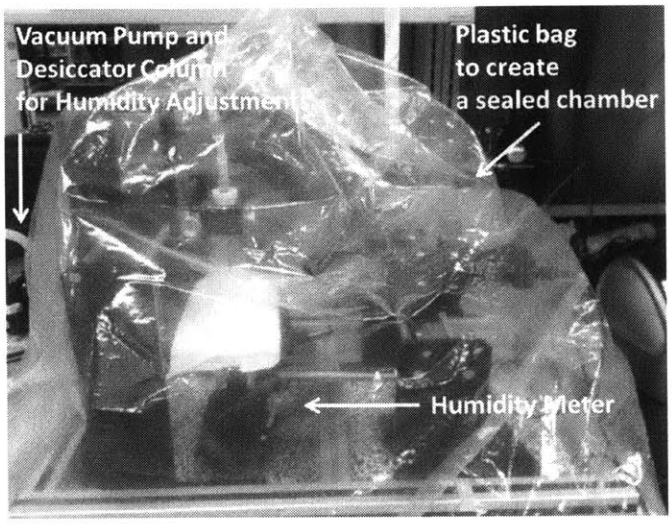

To introduce airflow into the system, a fan was placed on top of the tensiometer (Figure 5). This allowed for downward vertical airflow that mimicked the manufacturing conditions. The airflow speed, measured by a flow meter, was between 0.5 – 1 m/s.

Figure 5: Experimental Setup with Air Flow

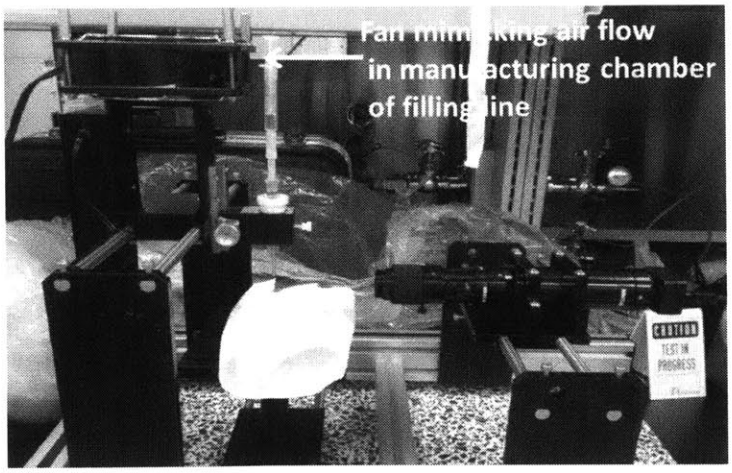

2.1.4.2.2 **Filling Study**

In addition to the tensiometer study, a few sets of filling experiments were completed to mimic integrated line studies and confirm the results from stoppage time studies. The study was done using the lab peristaltic pump to compare the drying time predicted by the tensiometer experiment. To represent all the parameters, 3 sets of conditions were used for the study, as shown in Table 7.

Table 7: Filling Experiments Used to Confirm Tensiometer Results

Experiment Number	Relative Humidity (%)	Air Flow from the Top (m/s)	Product Temperature (°C)	Nozzle ID (mm)	Concentration (mg/ml)
2	60	0.5	5	1	70
5	60	0	20	1	140
11	30	0	20	2.5	140

The standard operating procedure for the peristaltic pump usage was followed. For experiments 2 and 5, the following tubing set up was used: 1.2mm nozzle tubing, 0.8mm pump head tubing, and 1.0mm nozzle. For experiment 11, the following tubing set up was used: 1.6mm nozzle tubing, 3.2 mm pump head tubing, and 2.5 mm nozzle. Speed and acceleration were set at 200. Reverse levels were varied during the study to look at impact on droplet sizes. The experimental setups are shown below in Figure 6 and Figure 7.

Figure 6: Experimental Setup for Filling Study

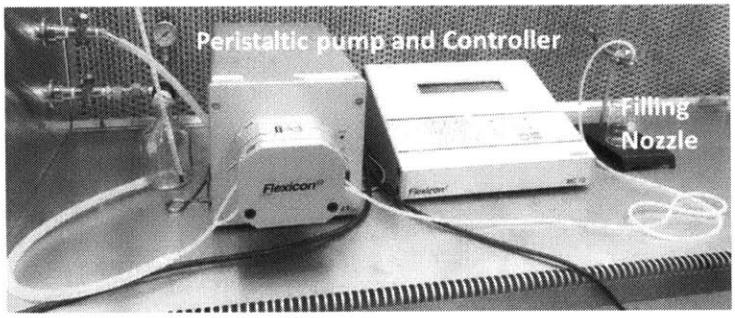

Figure 7: Experimental Setup with Reduced Humidity

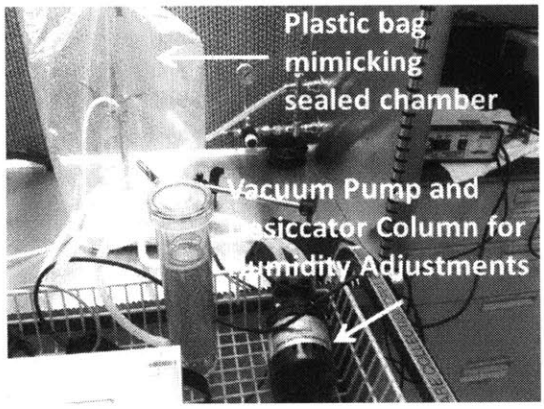

2.1.5 Results and Discussion

2.1.5.1 Model Results

Based on Ranz-Marshall correlations, drying rate from each experiment was obtained. Drying time was then calculated from the rate and critical concentration for each product. The results are indicated in Table 8.

Table 8: Drying Rates Obtained from Tensiometer Experiments

Experiment Number	Relative Humidity (%)	Air flow from the Top (m/s)	Product Temperature (°C)	Nozzle Inner Diameter (mm)	Concentration (mg/ml)	Drying Rate (Reduction in Volume) (mm^3/min)
1	30	0	5	1	70	-0.24
2	60	0.5	5	1	70	-0.11
3	60	0.5	20	1	70	-0.24
4	30	0	5	1	140	-0.26
5	60	0	20	1	140	-0.08
6	60	0.5	20	1	140	-0.24
7	30	0.5	20	2.5	70	-0.50
8	60	0	5	2.5	70	-0.14
9	60	0	20	2.5	70	-0.18
10	30	0.5	5	2.5	140	-0.60
11	30	0	20	2.5	140	-0.30
12	60	0.5	5	2.5	140	-0.44

2.1.5.2 Tensiometer Experimental Results

To visualize the surface tension of drug product droplet over time, tensiometer studies were performed. The correlation of dynamic surface tension (DST) and drying was first studied by Tripp et al. in 1995. However, the study looked at low concentration protein solutions. The study in this thesis focuses on high concentration protein solutions. A typical DST curve for a high concentration protein solution from our study is shown alongside Tripp et al. 1995 DST results for low concentration protein solutions in Figure 8.

Figure 8: Pendant Drop Results.

(A) Literature results of dynamic surface tension of low concentration protein solutions (Tripp et al. 1995). (B) Typical dynamic surface tension curve obtained using the FTA1000 pendant drop tensimeter

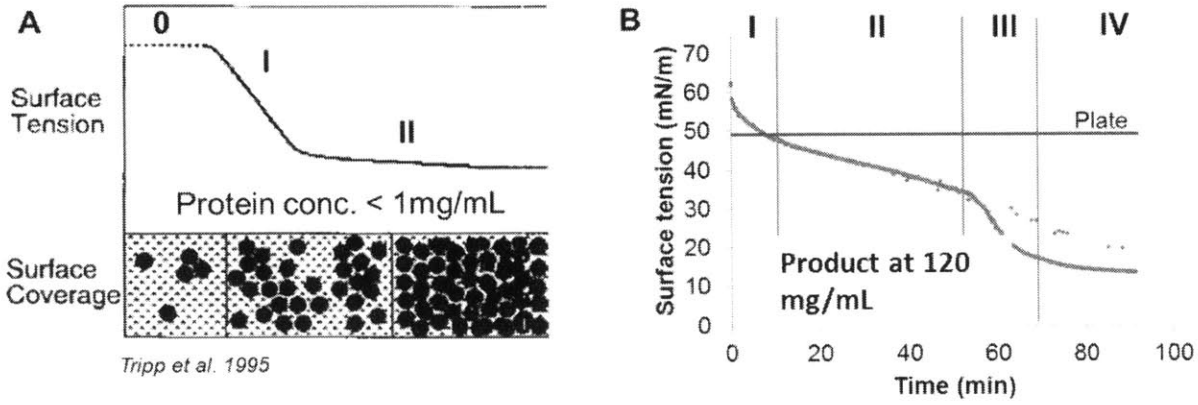

The DST results can be divided into the following phases (Beverung, 1999):

0 **Induction**: This phase is seen for low concentration protein solutions where there is low surface coverage at initial time points as protein has not yet diffused to the interface. Solutions with high protein/surfactant concentration do not exhibit this regime.

I **Rapid adsorption and surface coverage**: There is a quick drop in the surface tension as proteins and surfactant occupy >50% of the interface.

II **Mesoequilibrium**: In this phase the surface tension declines at a slower pace due to configurationally changes and unfolding of proteins at the interface. Evaporation also plays role in the drop of surface tension as the bulk protein concentration gradually increases.

III **Gel transition**: This phase is depicted by a second rapid drop in surface tension. We hypothesized that the protein solution droplet starts to transform into a viscoelastic gel at this point as it loses more moisture.

IV **Stable gel**: The surface tension and droplet volume do not change further in this regime. The droplet has very gel like appearance. The moisture is trapped in the center by several layers of protein.

Phases III and IV were seen in only high concentration protein solutions (70 mg/mL and greater). The phase behavior of DST curve is summarized in Figure 9.

Figure 9: Phase Behavior of Dynamic Surface Tension Curve

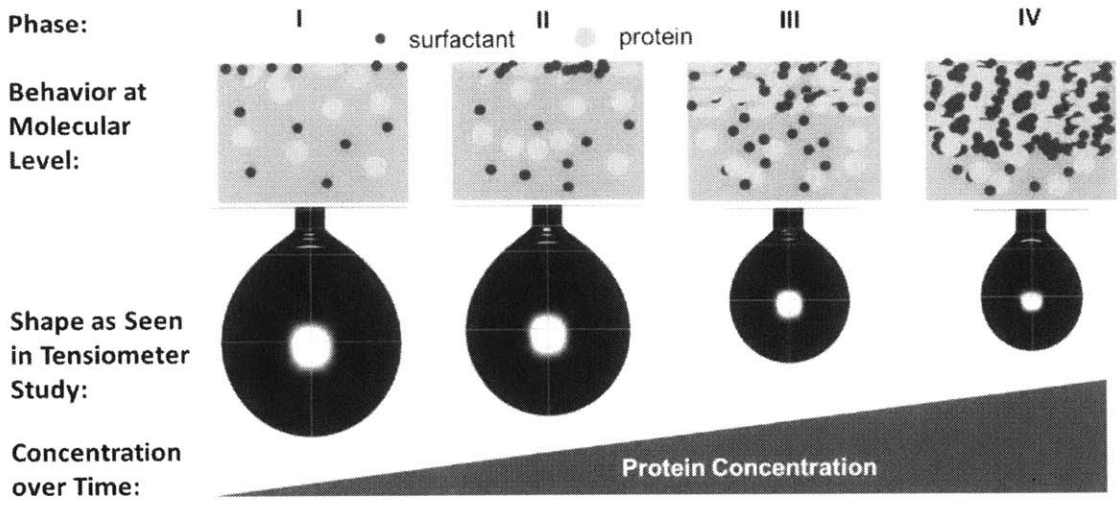

2.1.5.3 Correlation between Dynamic Surface Tension and Drying

We hypothesized that solutions that exhibit a second drastic drop in the dynamic surface tension with no further change thereafter (Phase III to IV transition) undergo drying/gelation. Drying is defined as the state in which the sample at the tip of the nozzle exhibits gel like characteristics. Applying extrusion force to the syringe at this stage will lead to splashing of the sample, if not complete blockage of the flow itself. To test our hypothesis, we first examined gelation in samples that did not exhibit Phase III to IV transition.

Figure 10 shows that Buffer, 1.1% CMC, and product at 0.5 mg/mL do not exhibit the Phase III-IV transition. The drop in surface tension seen at the end of phase II is a result of the ongoing evaporation and decrease in drop volume. In fact, the drop volumes decrease below 0.5µL between 70-90min for the samples. At this point, the drop sizes are too small for the instrument to produce a surface tension measurement. At the end of each run, extrusion force was applied to the syringe and the immediate flow from the needle was captured using a high speed camera. A clear stream of liquid was seen for all three samples, and the flow through the needle was not interrupted. Based on these results, we concluded that solutions that do not exhibit phases III and IV do not exhibit drying.

Figure 10: Dynamic Surface Tension and Drying Correlation for Buffer, CMC and Low Concentration Drug Product (0.5 mg/mL) Solutions Showing No Phases III and IV for Drying

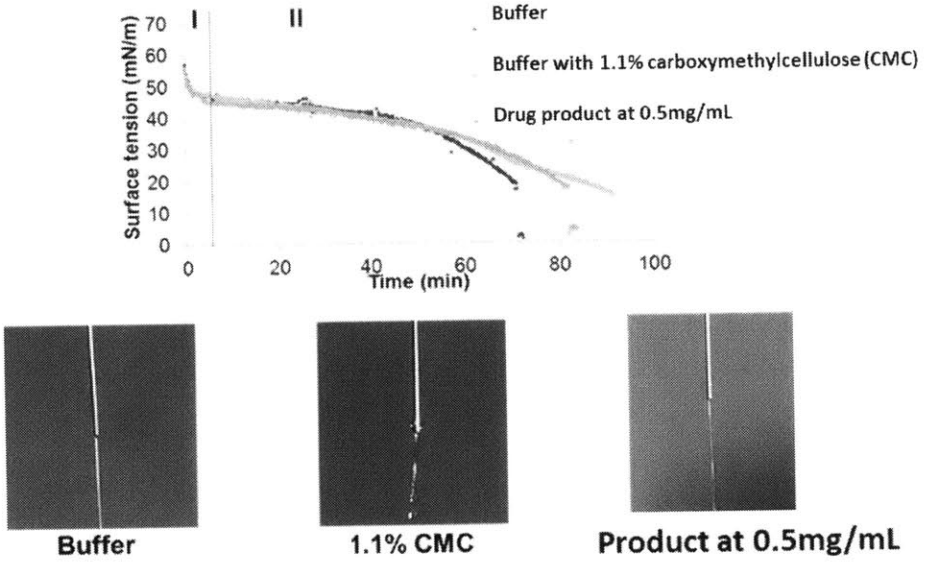

Filling Studies Showing No Flow Interruptions Caused by Evaporation in Buffer, CMC, and Low Concentration Protein Solutions

Next, we investigated drying in samples which showed the Phase III to IV transition. This transition was seen in drug product with concentration ≥ 70mg/mL. Extrusion force was applied at different time points which corresponded to the various phases on the DST curve. The flow images were captured with a high speed camera.

Figure 11 shows representative results for drug product at 70 mg/mL. A clean flow through is seen in Phase II which occurs at 45min since the drop was formed. At 63 min (Phase III) and 90 min (Phase IV), there was evident splashing as the sample flowed from needle. A semisolid gel like drop was also visible at the tip of the needle. The gel appeared to be more rigid at 90min, which was evident by the extreme splashing at this time point. Similar results were observed for the same drug product at 120 mg/mL and 140 mg/mL. However, the transition period was seen to shift to an earlier time point with increasing protein concentration (see below). Additionally, for higher product concentrations, there was complete blockage on flow in Phase IV. The results suggested that the start of Phase III of the dynamic surface tension data indicated the initiation of drug product drying on the needle tip.

Figure 11: Dynamic Surface Tension and Drying Correlation for Drug Product with Initial Concentration of 70 mg/mL Showing No Drying Until 63 Minutes

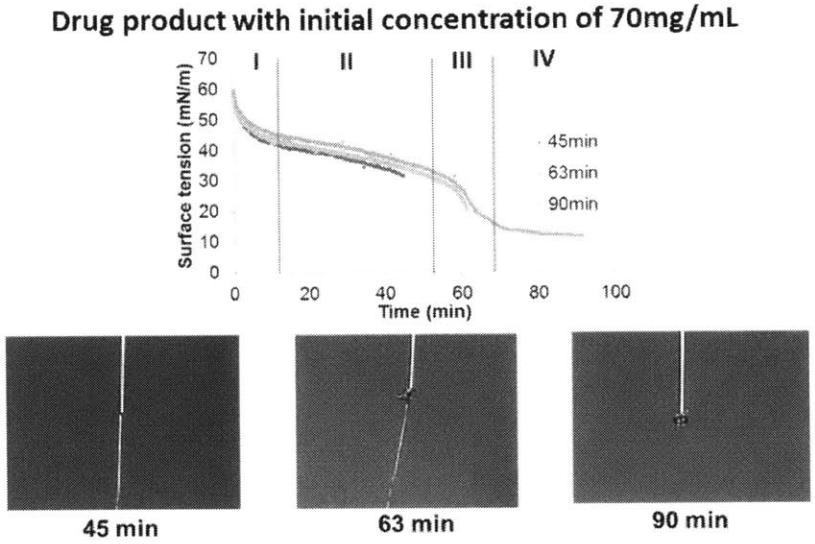

Filling Studies Showing Flow Interruptions Starting from the Beginning of Phase III

2.1.5.4 Tensiometer Drying Time Analysis

Surface tension of drug product droplet over time for each experimental set was graphed using Excel. The drying time, identified by the end of second phase of surface tension, was recorded.

Figure 12 shows an example of surface tension data plot (from Experiment 5); the drying time here is ~36 minutes.

Figure 12: Phase Behavior of Dynamic Surface Tension (DST) Curve

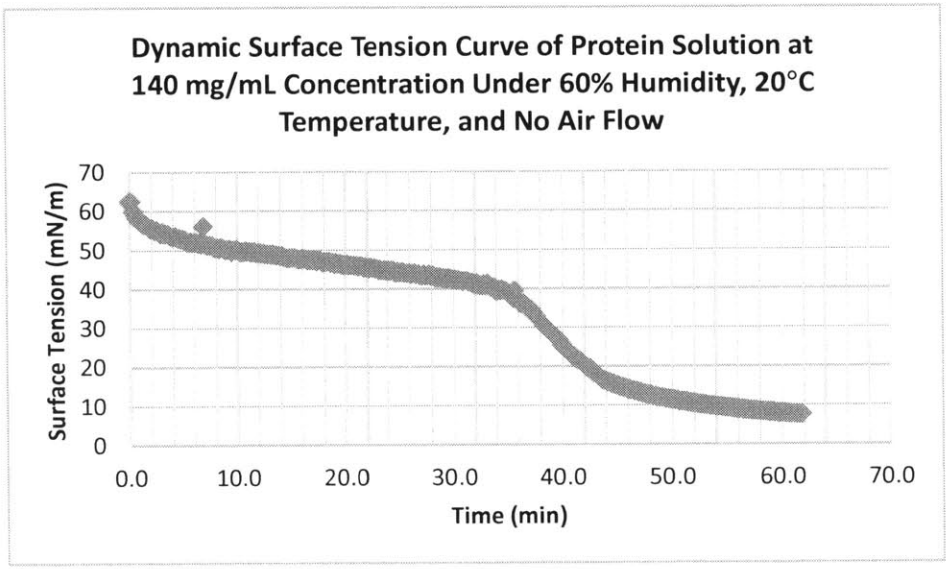

The volume of drug product droplet over time from the beginning to the end of phase 2 for each experimental set was also graphed. The drying rate was acquired by adding the linear trend line and identifying the slope.

Figure 13 shows an example of volume data plot (from Experiment 5); the drying rate here is -0.08 μL/min. The negative sign represents the reduction of droplet volume.

Figure 13: Drying Rate (Volume Reduction Rate) Plotted from Tensiometer Experimental Data

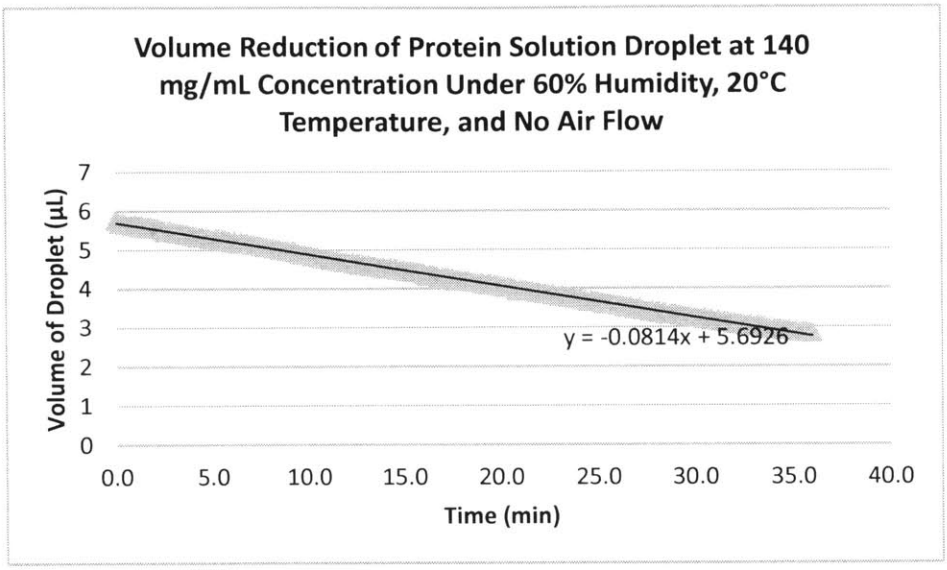

Protein concentration at the end of phase 2 was also estimated by dividing the initial volume of droplet to the initial product concentration and multiplying it with the volume at the end of phase 2.

Table 9 shows the drying time, drying rate and protein concentration of product at the end of phase 2 for each of the experimental setup. The experimental condition of each experiment is shown in Table 8 earlier.

Table 9: Results from the Tensiometer Study

Experiment Number	Drying Time as Represented by End of Phase 2 (min)	Drying Rate (µL/min)	Protein Concentration at the End of Phase 2 (mg/mL)
1	14	-0.24	192
2	15	-0.11	209
3	14	-0.23	151
4	10	-0.26	247
5	36	-0.08	283
6	6	-0.24	190
7	20	-0.50	167
8	100+	-0.14	214
9	100+	-0.18	170
10	14	-0.60	206
11	30	-0.30	250
12	18	-0.44	199

2.1.5.5 Comparison between Results from Predictive Model and Experiments

While the predictive model can be used to get drying rate, it requires critical concentration where gelation starts (between Phase II and III as discussed earlier) from the tensiometer studies. To get the model drying time, the average critical concentration from the experiments were used.

Figure 14 shows the critical protein concentration found across the experiments. On average, the drug product is considered dry at the critical concentration of 207 mg/ml, with standard deviation of 38 mg/ml, minimum of 151 mg/ml and maximum of 283 mg/ml. Discussion with formulation engineers showed similar level of variation found in the experiments.

Figure 14: Variations in Protein Concentrations End of Phase 2 across the Experiments

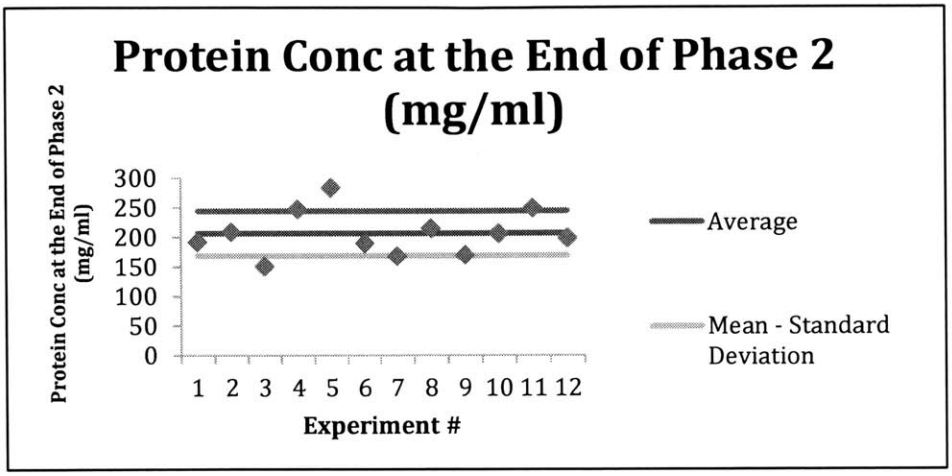

Results from predictive model and experiments were compared and showed that the model's predicted drying times were 1.5 minutes on average shorter than those from the experiments.

Figure 15: Comparison between Results from Model and Tensiometer Experiments

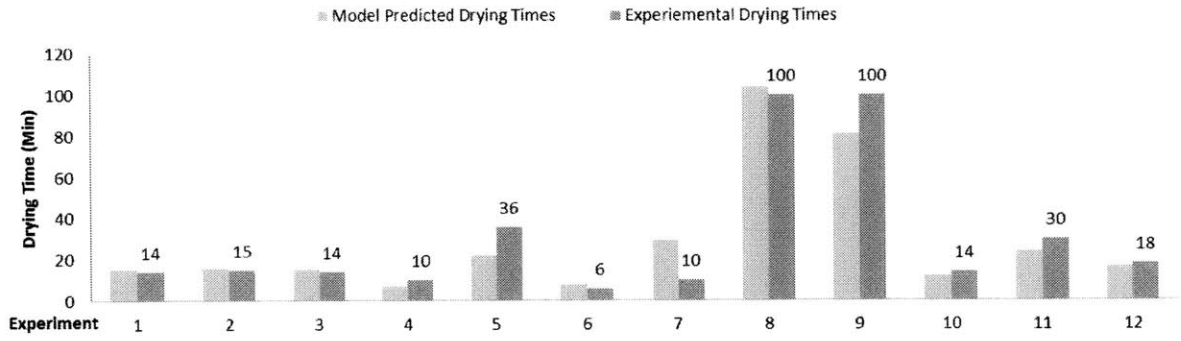

The raw data for Figure 15 are shown in the table below.

Table 10: Comparison between Results from Model and Tensiometer Experiments

Experiment Number	Experimental Drying Time as Represented by End of Phase 2 (min)	Model Drying Time (min)	Difference (min)	Adjusted Model Drying Time Based on Protein Concentration (min)	Adjusted Difference (min)
1	14	15.27	1.27	N/A	1.27
2	15	15.56	0.56	N/A	0.56
3	14	15.41	1.41	N/A	1.41
4	10	6.88	-3.12	9.26	-0.74
5	36	22.06	-13.94	34.25	-1.75
6	6	7.48	1.48	N/A	1.48
7	10	29.53	19.53	11.41	1.41
8	100	104.06	4.06	N/A	4.06
9	100	81.04	-18.96	N/A	-18.96
10	14	11.95	-2.05	N/A	-2.05
11	30	23.82	-6.18	32.47	2.47
12	18	16.23	-1.77	N/A	-1.77

Much of the differences in drying time were due to the variation in critical protein concentration. Adjusting for data points where the critical concentrations resulted from the experiments were significantly different from the average, with the variation between model and experimental results being 1 minute on average with standard deviation of 6 minutes.

2.1.5.6 Statistical Analysis of Data and Development of Predictive Model

The correlation between drying times of model and experimental conditions was studied using JMP® Statistical Analysis tool. The model showed that the five

experimental conditions can cover 87% of variations in drying times (shown by RSquare Adj value of 0.871178, Figure 16).

Figure 16: Response Drying Time (End of Phase 2)

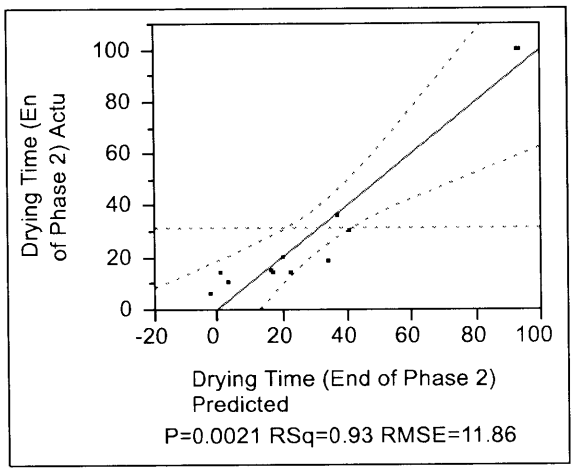

Summary of Fit

RSquare	0.929734
RSquare Adj	0.871178
Observations (or Sum Wgts)	12

The effects of relative humidity, air flow, nozzle inner diameter, and product concentration on drying times were considered statistically significant as shown by p values of <0.05 (95% confidence level, Table 11). The effect of product temperature on drying time is not considered statistically significant.

Table 11: Analysis of Variance

Source	DF	Sum of Squares	Mean Square	F Ratio
Model	5	11179.970	2235.99	15.8779
Error	6	844.946	140.82	**Prob > F**
C. Total	11	12024.917		0.0021*

The effect of relative humidity on drying time was shown, as the lower level of humidity (30%) reduced the time it takes to dry. Similarly, increased air flow also reduced the time it took to dry.

Product temperature did not significantly affect drying time. This could be explained by the fact that the product temperature changes over time due to the difference in temperature between product and environment. Because the amount of drug product at the end of the nozzle was small, the time it took for product temperature to match that of the environment was insignificant when compared to the time it took for it to dry.

Nozzle size also has an impact on drying time. Larger nozzle size provided a larger surface area, making it take longer to dry. Lastly, the initial protein concentration played a role in the drying time as lower initial concentration takes longer to get to the critical concentration, leading to a longer time to dry.

Figure 17: Prediction Profiler Showing Effects of Different Parameters on Drying Times

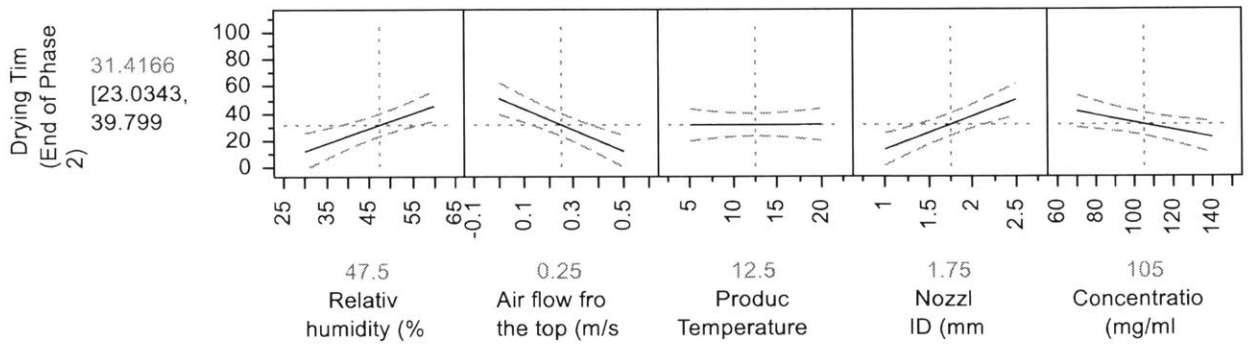

2.1.5.7 Filling Study

The filling study showed similar results with gelation observed in the tensiometer experiments. The study also showed that the size of the droplet as set

by the reverse setting on the peristaltic pump matters greatly for drying time. The larger droplet, the longer it takes to dry. Complete suck back also helps extend the drying time.

Different reverse settings were used to understand the impact of droplet sizes. A visual as shown below in Figure 18 was used to score droplet sizes left at the filling nozzle at line stoppage under different reverse settings. The droplet sizes used during the tensiometer study were about score #3 in the figure, showing about half of the droplet hanging outside the filling nozzle.

Figure 18: Droplet Sizes

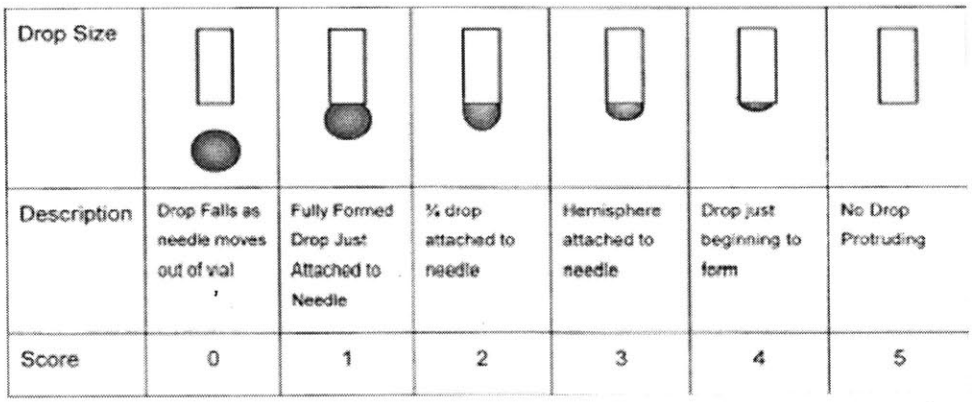

Amgen, Inc

Table 12: Experiment 2 Conditions (Predicted Drying time of 15 Minutes)

Reverse Setting	Droplet Size	Time left to dry (min)	Observations
0	~ The same size as in tensiometer study (about #3)	15	Gelation. 6-7 flushes
1	Very small (#4)	15	Drying. 10X flush to back to normal
1	Very small (#4)	10	Drying. 5X flush to back to normal
3	Suck-back (#5)	15	No drying

Table 13: Experiment 5 Conditions (Predicted Drying time of 36 Minutes)

Reverse Setting	Droplet Size	Time left to dry (min)	Observations
0	Larger than tensiometer study (#2)	25	No drying
0	Larger than tensiometer study (#2)	40	No drying
3	~ The same size as in tensiometer study (about #3)	30	No drying
3	~ The same size as in tensiometer study (about #3)	36	Gelation. Fills not straight down but not splashy either. Video captured.
3	~ The same size as in tensiometer study (about #3)	40	Drying. Splashing to ~60 degree angle. Not recoverable after 20 flushes. Video captured.
5	Suck-back (#5)	35	No drying

Table 14: Experiment 11 Conditions (Predicted Drying Time of 29 Minutes)

Reverse Setting	Droplet Size	Time left to dry (min)	Observations
0	~ The same size as in tensiometer study (about #3)	30	Drying, 1 flush
1	Suck-back (#5)	30	No drying

2.1.6 Conclusion and Recommendations

Studying how different variables impact drying is important for process development. In manufacturing, fill weight checks and other stop reasons may lead to product drying at filling nozzles. It is thus critical to understand the maximum stoppage time of a filling line before drug product drying becomes an issue, so that the number of rejected vials and syringes can be minimized. In the pre-commercial

phase before production is selected, many sites have humidity and air flow restrictions; it is important to understand what those restrictions are and how they affect manufacturability.

The link between tensiometer results and confirmation with filling studies showed an effective correlation and ability to use tensiometer as a more cost-effective method to study drying times.

We were able to leverage the Ranz-Marshall mass transfer correlation and tensiometer experiment to limit the onsite integrated line study to get the maximum stoppage time before drying becomes a problem during the filling process. This approach reduces cost and resource requirements associated with onsite integrated line study. Additionally, it provides increased flexibility as the study no longer requires dedicated integrated filling line time, allowing the study to be done in an earlier phase of development before manufacturing site selection is complete. Lastly, because the First Principles predictive model identifies and key parameters that influence drying times, increased process understanding can be gained. The knowledge from the model can be useful in developing manufacturing site selection criteria as well as in problem troubleshooting on the manufacturing line.

It is recommended that a set of three tensiometer experiments per drug product to be used to get the average critical concentration and the First Principle predictive model to determine the maximum drying time.

2.2 Applying Computational Fluid Dynamics (CFD) to Study Parameters Affecting Drug Product Filling Unit Operations

2.2.1 Project Summary

A phenomenon that leads to increased reject rates and decreased yields during filling is dripping. Because each fill takes less than one second, it is difficult to visualize the phenomenon as it happens and to identify parameters that cause it. We present the application of Computational Fluid Dynamics (CFD) in understanding the relationships between drug product attributes and operating parameters and in predicting the quality of fill as indicated by dripping.

CFD is a branch of fluid mechanics that uses First Principles numerical methods and algorithms to solve and analyze problems involving fluid flows. Because it applies First Principles, it enabled us to identify key drug product attributes and operating parameters that can affect the dripping phenomenon. For these parameters, a Design of Experiments (DOE) was developed to study each parameter's effect on dripping. The geometry of the filling nozzle and drug product syringe was modeled on the CFD software and the parameters from each set of DOE were inputted. CFD computes mass transfer across the geometry to help visualize each fill. At the end of each CFD experiment, the dripping phenomenon was recorded.

Laboratory-scale filling experiments were performed to compare the results of the CFD model and to confirm that the model is a good representative of the filling process seen in the real world. After the confirmation, the CFD model was identified as a good preliminary tool for use in optimizing parameters to prevent

dripping. Using the CFD model, the researchers could predict whether dripping would likely be seen during engineering run and how the parameters should be adjusted to minimize the probability of dripping. Oftentimes, engineering runs had to be repeated due to the dripping phenomenon. The model made it less necessary to rely on trial and error in order to get the parameters right the first time and to minimize dripping during engineering runs on manufacturing lines.

2.2.2 Project Introduction

Most large-molecule protein and vaccine biopharmaceutical drug products are delivered by injection and thus require aseptic liquid filling into vials and syringes. Piston pumps, which are mechanical devices that cycle through a suction and a pressure phase to move fluid, have been a traditional liquid-filling technology in biopharmaceuticals, but increasing focus on contamination prevention as well as technological advancements in peristaltic pumps' speed and precision have led manufacturers to consider peristaltic pump filling technology in recent years (Lambert, 2008).

Unlike piston pumps, which require that their internal parts (e.g., gaskets, seals, valves, and internal surfaces) be in direct contact with the fluid, peristaltic pumps continuously apply external pressure to a silicone tube to move fluid, allowing the pharmaceutical-grade tubing to be the only parts that come into contact with drug products. As a result, peristaltic pumps can be used for single-use aseptic filling and reduce the risk of cross-contamination between batches.

While studies on the impact of drug product quality (such as shear impact) during the filling process have been done, publications related to the manufacturing challenge in filling of high-viscosity monoclonal antibody formulations are still limited, especially for the peristaltic pump filling technology (Shieu, 2014). As drug products are designed to be more concentrated to minimize dosing for patients, viscosity of products becomes a concern for peristaltic pump filling process, as the pumps apply only a marginal pressure.

As more products are being filled with the peristaltic pump technology, the relationships between drug product attributes properties (e.g., density, viscosity, concentration, surface tension, contact angles with nozzle/primary container) and operating parameters (e.g., speed, acceleration, reverse, line speed, nozzle starting position, nozzle movement speed, nozzle/tubing sizes) must be understood to ensure the manufacturability. Generally, scientists optimize the parameters using scale-down models and repeat the experiments again in the manufacturing environment. Such approach requires time away from clinical and commercial fills and is limited in ability to provide information on design space, as experiments take a long time and each fill takes only less than one second, making its quality difficult to observe.

Three general phenomena that lead to increased reject rates and decreased yields during filling are dripping, splashing and foaming (Figure 19). Dripping refers to drug product leakage from the nozzle after the target fill has been achieved. Drug products with either high viscosity and/or low surface tension with the nozzle are

most susceptible to dripping. Foaming may be observed at the surface of the drug product after it has been dispensed into the primary container. Formulations with high protein concentration and/or high surfactants are more prone to foaming. Lastly, splashing is observed on the inside wall of the primary container and is often a result of high fill speed, nozzle movement, or contact angle between the drug product and vials/syringes. These phenomena are very common during the process development when the process parameters have not been optimized to the drug product attributes (e.g., density, viscosity, concentration, surface tension, contact angles with nozzle/primary container). Encountering these problems during the engineering runs, which require integrated filling line time, is costly in terms of resources and takes away time that the manufacturing line could be used to produce products. Additionally, because the filling process happens at such a high speed (<1 second per vial/syringe), it is difficult to troubleshoot the problem on the line with naked eyes.

Figure 19: A Cartoon Depiction of A. Standard Fill and Process-Associated Challenges (B. Dripping, C. Foaming, and D. Splashing)

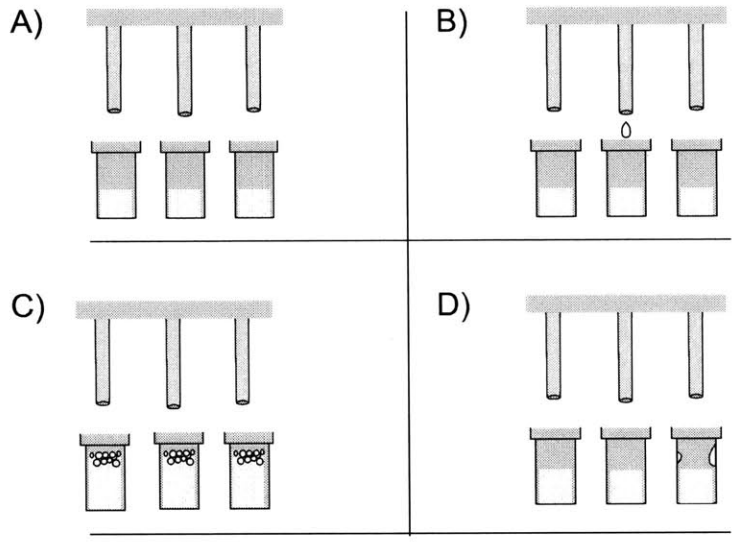

2.2.2.1 Project Approach

We present the application of Computational Fluid Dynamics (CFD) in understanding the relationships between drug product attributes and operating parameters and in predicting the quality of fill as shown by the three general phenomena mentioned above. CFD applies the First Principles to help with visualize these phenomena. To understand the model's ability to mimic the filling process, the Design of Experiments was used to compare phenomena in the model to those of actual filling experiments.

2.2.3 Background Information

2.2.3.1 Peristaltic Pump

Figure 20 shows the basic schematic drawing of a peristaltic pump filling process. The drug product in the surge vessel passes through surge vessel tubing before being moving through a reducer and hybrid tubing. The surge vessel tubing

is typically much bigger in diameter than that of the hybrid tubing to prevent pump cavitation and backpressure. The drug product flowing through the hybrid tubing is then split into 2 streams using a Y-connector and pump head tubing. Peristaltic pumps used for biopharmaceutical filling require fill accuracy that can be achieved by more complex configurations. To reduce pulsation (variation of product volume passing through the pump at a given time) and improve fill accuracy, the number of rollers is increased. Due to limited room for rollers inside the pump, double rotor with six rollers each and placed offset with respect to one another are used. Each stream of drug product in pump head tubing passes through one rotor in the pump before coming back together after with another Y-connector and hybrid tubing. The hybrid tubing is connected to a nozzle, which fills drug product to vials and syringes. In between each fill, the flow is stopped by spring mechanism pinching the pump head tubing on either side of the pump to restrict the flow.

Figure 20: Basic Schematic Drawing of a Peristaltic Pump Filling Process

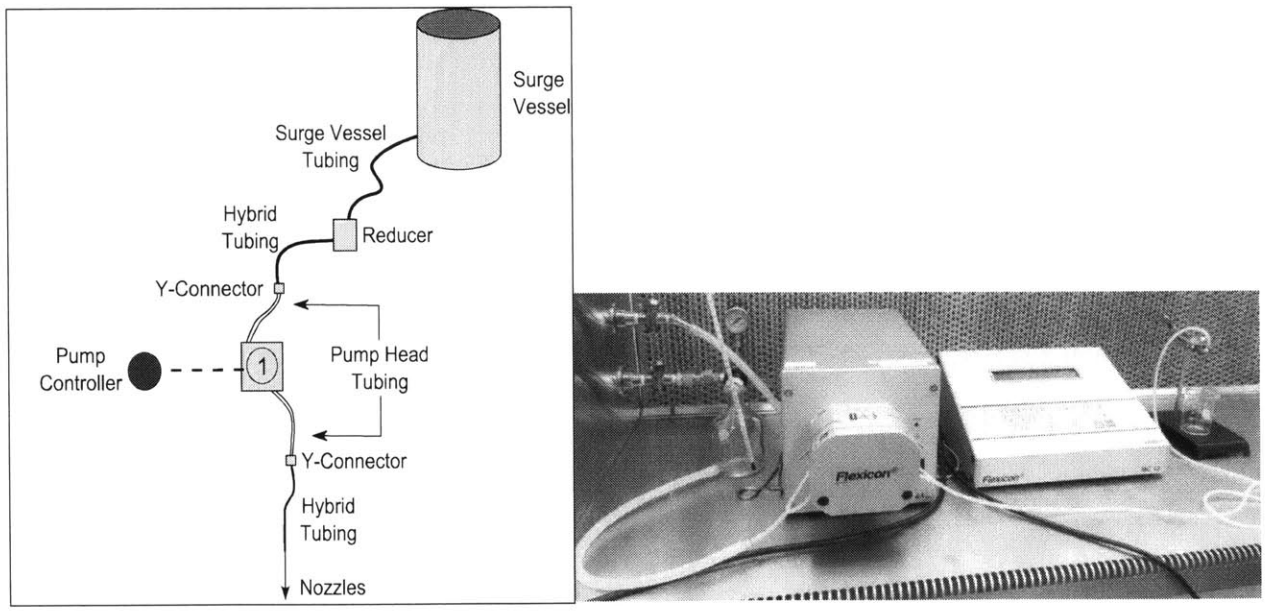

Peristaltic pumps can be controlled in speed (rpm), acceleration (and deceleration), and reverse settings. Depending on fill volume for each vial or syringe and accuracy needed, a pump head tubing size is chosen. As the pump rotor turns, the rollers occlude part of the tube forcing the fluid to be pumped through the tube. The flow rate of the pump is directly related to the diameter of the tube and the speed of rotation. The acceleration (and deceleration) determines how fast the pump rotors get up to the designated speed (and back down to zero). Flexicon PD12 I Series B peristaltic pump has an acceleration rate setting between 1 and 200 (dimensionless proprietary setting from Flexicon©), with higher values translating to faster acceleration rates. The deceleration rate is equal to the acceleration rate. The faster the deceleration translates to the less chance of drug product dripping at the end of the fill. However, the time to which each deceleration rate corresponds is not known. The peristaltic pump also has a reverse parameter settings from 0 to 10 controlling the back rotation of rotors after each dispenses, with 1 equals to a 12 degree turn. The reverse setting is used to bring liquid back inside the nozzle reducing the chance of dripping between each fill and exposure to the environment during stops.

In the manufacturing environment, peristaltic pump filling is scaled up in a trolley configuration and with up to 10 heads (Figure 21). The surge vessel is connected through a manifold to up to 10 peristaltic pumps in the similar manner as discussed above. The number of pump heads used is dependent on the number of primary containers per row in the filling nest. A typical syringe nest contains 10 syringes per row and CZ-cartridges have 8 per row, in these instances either 10 or 8

heads would be used, respectively. Line speed is set based on the filling flow rate. The nozzles also move up and down at a speed setting.

Figure 21: Peristaltic Pump Filling Configuration in Manufacturing Environment

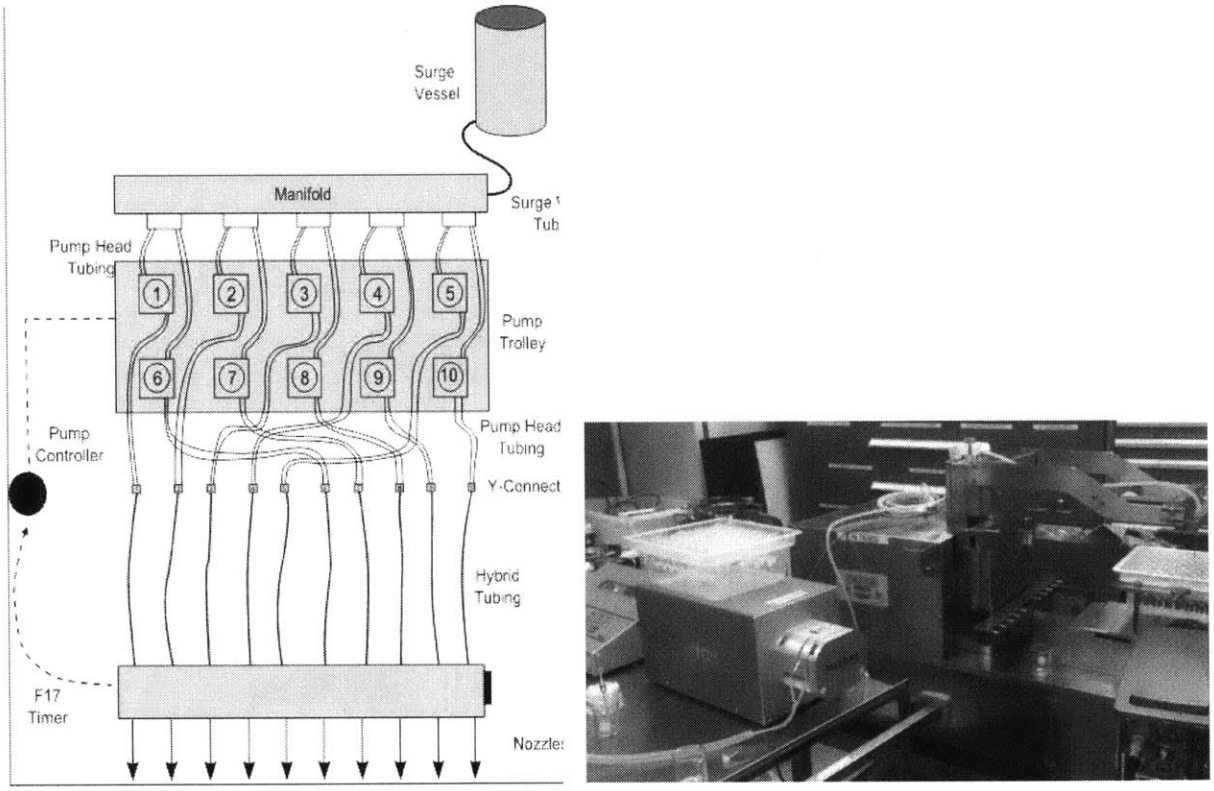

2.2.3.2 Computational Fluid Dynamics (CFD) Study of Peristaltic Pump Filling

CFD is a branch of fluid mechanics that uses numerical methods and algorithms to solve and analyze problems involving fluid flows. It is fundamentally based on the Navier-Stokes equations, which describe the motion of fluid. Coupled with fluid flow are additional physical and/or chemical processes: e.g., multiple phase (gas-liquid or solid-liquid or solid-liquid-gas) interaction, species transport, heat transfer, mass diffusion, and chemical reactions (Wilkes, 2005).

CFD technology is well established in the aerospace and automotive industries, and it entered the chemical industries in the past decade. Recently, the pharmaceutical industry has shown increased an interest in CFD for providing insight into fluid flow and related phenomena that can help mitigate risks associated with scale-up of process equipment as well as troubleshooting. The accuracy of CFD model predictions depends on computational numerical precision, model input data accuracy, and scientific understanding of the governing laws and the nature of fluids (Pordal, 2002).

2.2.4 Materials and Methods

2.2.4.1 Geometry for CFD Modeling

The Ansys Inc's Gambit preprocessor was used to model the geometry used for CFD modeling of the filling process. Because the three phenomena all involved the filling nozzle, we restricted the boundary to the filling nozzle and the primary container (syringe, in this case). The initial model included the geometry a stainless steel filling nozzle with a diameter of 1.6mm and height of ~107.3 mm and a glass syringe. Figure 22 shows the geometry created.

Figure 22: Geometry of CFD Model for Filling Process

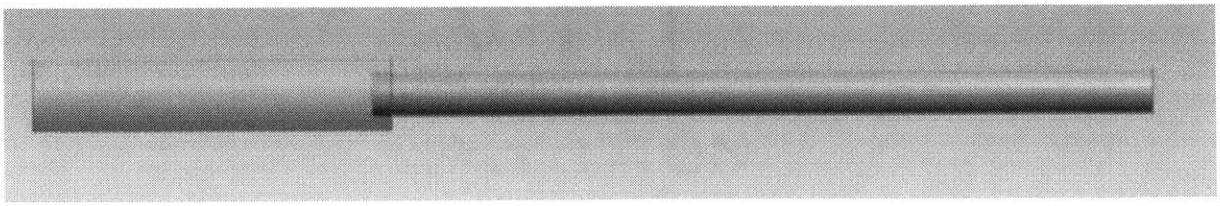

2.2.4.2 Meshing of Geometry for CFD Modeling

The geometry was then divided into small structured hexagon cells in a process called meshing with resolution in the order of 40 μm. Because fundamental fluid mechanic equations would be solved in each individual cell in the resulting mesh, the cells were divided even more to the order of 8μm at the walls where the phenomena were likely to be observed. Figure 23 shows the meshing of the geometry.

Figure 23: Meshing of Geometry Used in CFD Modeling

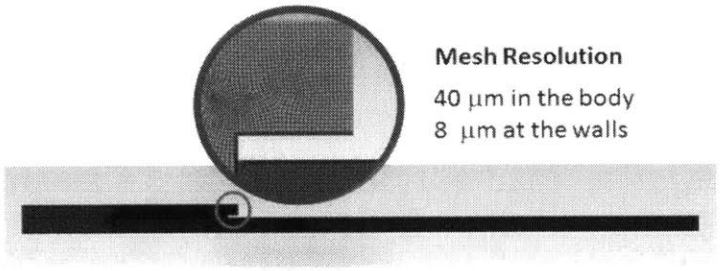

2.2.4.3 CFD Modeling

The commercial software developed by Ansys, Inc. called Fluent version 14 was used to perform the CFD simulations. In the CFD model, equations (including Navier-Stokes and Species Transport) were numerically solved in an iterative fashion by the software. Solution data were subsequently processed to determine the distribution of all the fluid mechanical properties (including flow and species mass fraction) from nozzle to syringe. Flow distribution profiles were obtained for regions of interests.

2.2.4.3.1 Inputs for the CFD Model

Fluid properties and operating parameters were inputted into the CFD model. The fluid properties include density (kg/m^3), viscosity (kg/m-s), surface tension (N/m), and wall adhesion angles of fluid to nozzle as well as primary container. These properties were obtained experimentally during drug product characterization studies.

Mass flow rate (kg/s) at a given time was also required for CFD modeling. For the peristaltic pump technology, volumetric flow rate equals to liquid volume in tubing between rollers x number of rollers x roller speed. The controller of Flexicon PD12 I Series B calculates the steady state volumetric flow rate automatically from the pump head tubing inner diameter size (mm) and speed (rpm) inputs. The mass flow rate could then be obtained by multiplying the volumetric flow rate by the drug product density. Table 15 shows the list of inputs to the CFD model for filling.

Table 15: Inputs to the CFD Model for Filling

Input	Category
Density (kg/m3)	Fluid Property
Viscosity (kg/m-s) at 5C	Fluid Property
Surface Tension (N/m)	Fluid Property
Wall Adhesion Angle of Fluid to Nozzle	Fluid Property
Wall Adhesion Angle of Fluid to Primary Container	Fluid Property
Mass Flow Rate (kg/s) at a Given Time	Operating Parameter

2.2.4.4 Design of Experiments

After the CFD model was set up, a set of experiments were used to test the model (Table 16).

Table 16: Design of Experiment for CFD Model

Experimental Number	Viscosity (kg/m-s)	Drug Product Surface Tension (N/m)	Wall Adhesion Angle to Nozzle (°)	Wall Adhesion Angle to Syringe (°)	Nozzle Size (mm)	Steady State Flow Rate (mL/sec)	Deceleration Time (sec)	Reverse Time (sec)
1	0.0145	0.048	80	40	1.6	20	0	0
2	0.0145	0.048	80	40	1.6	50	0.02	0.2
3	0.0145	0.048	80	40	1.6	120	0	0
4	0.0145	0.048	80	40	1.6	120	0.01	0
5	0.0145	0.048	80	40	1.6	120	0.02	0
6	0.0145	0.048	80	40	1.6	120	0.04	0
7	0.0145	0.048	80	40	3.2	320	0.02	0
8	0.0068	0.043	80	40	1.6	120	0.02	0

2.2.4.5 Experimental Setup for CFD Model Validation

Table 17: List of Materials and Equipment for the Filling Study

Component/ Equipment	Equipment Number
Drug Product at 105 mg/mL	Amgen, Inc.
250ml Surge Vessel	KIMAX
3/8" Tubing	Accusil
1.2mm Tubing	Accusil 84-103-012
0.8mm Tubing	Accusil 84-103-008
Y Connector	Accusil 84-012-002
1.6mm Filling Nozzle	Flexicon 30-030-016
Peristaltic Pump	Flexicon 61-150-022
High-Speed Video Camera	Olympus iSpeed TR

2.2.4.5.1.1 Setup

One difference between the peristaltic pump setup in the lab and clinical manufacturing scale is the use of a manifold upstream of the pump head in manufacturing (Figure 21), whereas the scale-down lab scale uses the upstream Y-connector that splits into the two pump head tubings (Figure 20). In order to mimic

the clinical manufacturing scale, a mini-manifold was used. The updated scale-down model with the "mini-manifold" is shown in the images below.

Figure 24: Mini-Manifold Set Up in the Lab Environment

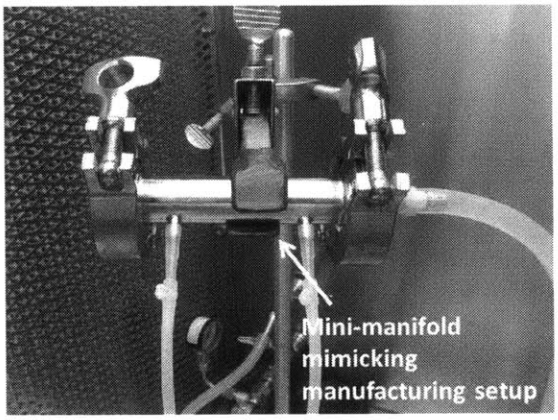

2.2.5 Results and Discussion

2.2.5.1 Results of Model for Dripping Phenomenon

The CFD model was run under the conditions presented in the Design of Experiments. Table 18 provides information on whether or not dripping was observed.

Table 18: Results of the CFD Model

Experimental Number	Dripping?
1	Yes, all drips
2	Yes
3	No
4	No, but almost
5	Yes
6	Yes
7	No
8	No

A key takeaway from the results was that faster deceleration leads to a smaller droplet formation and less dripping after each fill. However, at a slow

deceleration rate (0.04 sec here), the droplet falls off at the end, leaving no droplet at the nozzle. This could explain the reduction in dripping seen when acceleration was reduced from 200 to 50 during the engineering run in the clinical manufacturing.

Figure 25: Effect of Deceleration on Dripping Phenomenon as Shown by Instantaneous, 0.1, 0.2, and 0.4 Seconds Deceleration

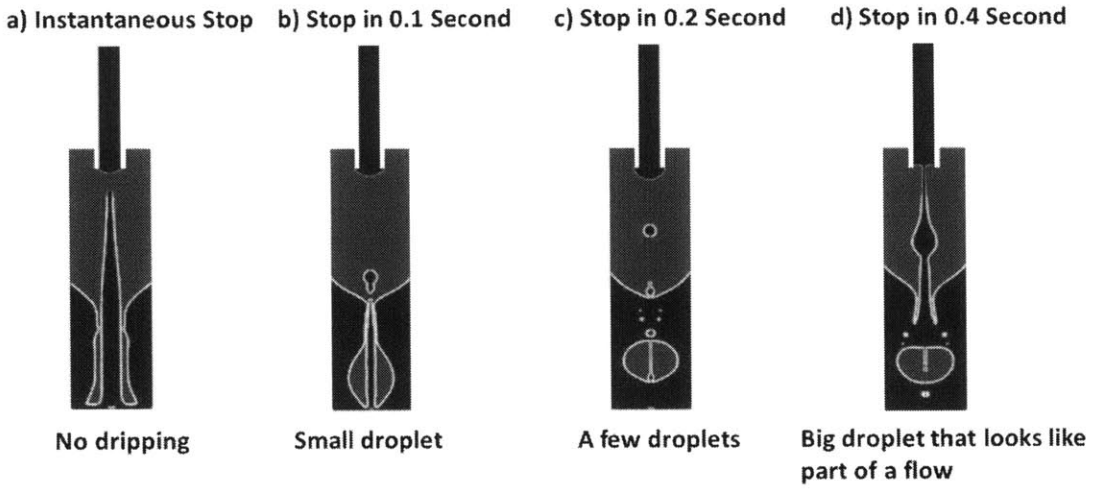

The model also showed that dripping happens during both deceleration and reverse. For viscous products filled with a large diameter nozzle, there is a risk of dripping even with fast deceleration (Figure 26).

Figure 26: Fluid Flow during Fill, Deceleration, Stop, and Reverse

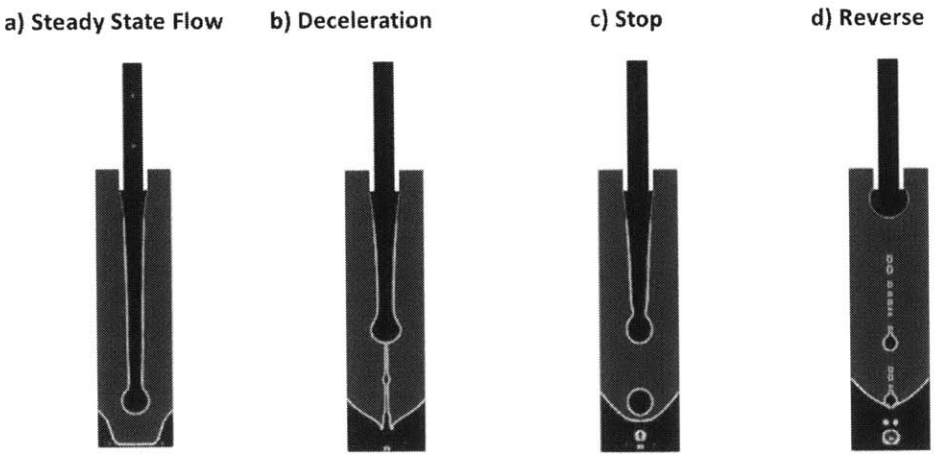

2.2.5.2 Experimental Confirmation of Model for Dripping Phenomenon

2.2.5.2.1 Confirmation of Boundary Condition

Because our CFD model has a boundary from the nozzle to syringe, leaving the upstream equipment out of the focus and only considering it through flow rate into to the model, a study was performed to confirm that the upstream pressure would not significantly affect dripping downstream when the tubing is pinched by the intervening pump head. Two sets of experiments were performed in order to compare filling - the first with 105 mg/mL drug product fed into the mini-manifold with no pressure on the surge vessel, and the second with the same set up with a 10 psig pressurized stainless steel surge vessel. Please note that 10 psig is significantly higher than observed in manufacturing (< 1 psig). Figure 27 shows the experimental setup of pressurized vessel.

Figure 27: Experimental Setup for Pressurized Vessel

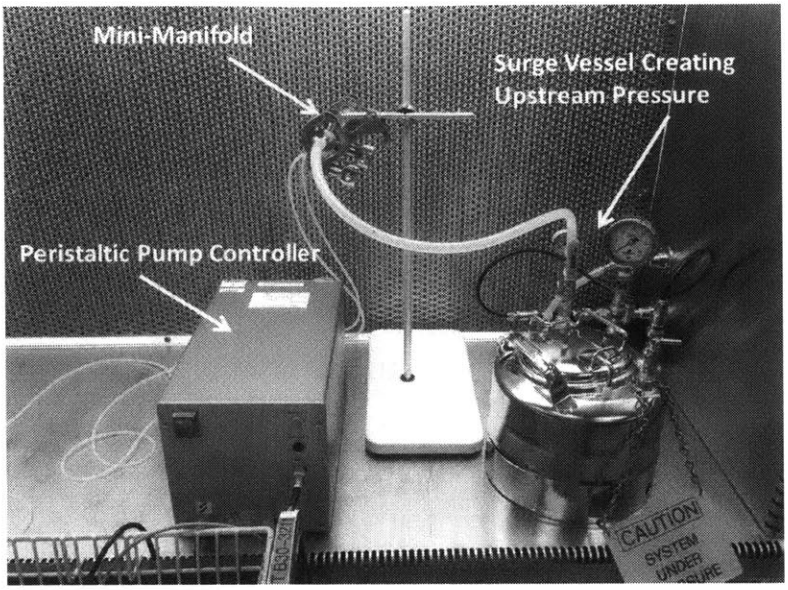

The experiment showed that upstream pressure can cause the dripping phenomenon to happen more often.

2.2.5.3 Discussion

The CFD model of filling showed that faster deceleration leads to a smaller droplet formation and less dripping after each fill. However, even at a deceleration rate of 0.02 seconds (relatively instantaneous), the dripping was observed for a drug product with 14 cP viscosity filled with 1.6mm nozzle. Typically, tubing size for peristaltic pump filling is chosen based on fill volume, and nozzle size is of a similar size. The CFD model suggested that this approach may not be feasible for high concentration/viscosity products. The relationship between viscosity and nozzle size with respect to dripping was also studied further.

2.2.6 Conclusion and Recommendations

CFD can be used help visualize phenomena that are difficult to observe in real time. In the case of the filling process, we were able to use it as a tool to investigate parameters affecting the dripping phenomena.

CFD was not without limitations, however. In our case, the dripping phenomenon observed in the model and experiments was used as a pass/fail gate to validate the model. We did not have a quantitative comparison. This limited us from using the CFD model to significantly reduce the number of experiments. The model was used to help improve process understanding by helping us understand the key parameters causing dripping.

The decision to not have a quantitative measure such as fill weight was made because of the computational time. To simulate the deceleration required two days of computational time for each experimental set. Computing the entire fill would exceed computational power and extend the time significantly. Additionally, the filling process included flexible tubing which is a non-deterministic parameter. CFD assumes that all parameters are deterministic. If we used a quantitative measurement, it would be difficult to distinguish error caused by the non-deterministic nature of the tubing from that caused by the difference between the model and the experiment.

Nevertheless, the CFD can be a powerful tool in process design. Before committing to the use of first principles and computational fluid dynamics modeling, a prioritization of key unit operations to leverage the approach should be completed

to ensure that resources and expectations are met before the work begins. To do so, key criteria to select future potential candidates for first principles modeling are established to provide framework for cost/benefit analysis.

Table 19 and Table 20 provide key considerations into how topics to apply first principles modeling should be chosen and how their benefits should be evaluated. They take into account the limitations that first principles model have and can help align expectations before committing to using the models to reduce or eliminate experiments.

Table 19: Criteria for choosing topics to apply first principles modeling

Science	• Is the science there? • Can all the variables be captured in governing equations?
Scalability	• Are differences across lab to manufacturing scales and technology platforms well understood? • Would separate models be needed for different platforms?
Quantitative Comparison between Model and Experiment	• Can the governing equations be solved in a reasonable amount of time utilizing current analytic tools? • Are there defined acceptable ranges for parameters to compare the model and experiment? • Are variations in outputs of experiments understood?

Table 20: Criteria for evaluating the benefits of first principles modeling

Cost	• How much resources (headcount, raw materials) are required? • What is the variation in study from one product to another?
Quality	• How much waste in manufacturing process is currently due to lack of design robustness? • Would the model allow for a more holistic understanding?
Speed to Market	• Does the current study require line time or constraint resources? • Are there significant risks associated with engineering runs?

2.3 Leveraging Data Generated at Clinical Scale through Process Monitoring to Illustrate Improvement Opportunities and Highlight Risks

2.3.1 Project Summary

This project was intended to be used as the starting point for cross-product data review in clinical manufacturing. Comparing the data across different products can illustrate improvement opportunities and highlight risks. It can drive learning across product teams, catch weak signals that appear repeatedly but that are not at non-compliance limits in individual settings, and provide data-driven culture for continuous improvement. For instance, product A may have a much higher scrap rate than product B. Comparing them together may enable us to troubleshoot more quickly what the root cause of the high scrap may be. This is particularly important in the phase of clinical manufacturing where products are not yet being produced in a large scale, meaning that there is still room for process adjustments.

We used inspection data as an initial focus for cross-product review. Two years' worth of inspection data were collected and categorized by types of containers as well as by reasons for rejects. Statistical analysis tools were used to set upper control limits for each. New inspection data across products were collected monthly and the combined results were trended against the limits. The trends were measured against Nelson violations, which are 1) a point above upper control limit, 2) nine or more points in a row above the mean, 3) six or more points in a row continually increasing, or 4) fourteen or more points in a row in alternating direction (increasing then decreasing). Root cause analysis was then implemented for products that showed signs of violations. Investigations were performed by representatives from Process Development, Manufacturing and Quality.

In the three months of the pilot program allowed for establishment of system that could help identify cross product trends. In the example of the inspection procedure training, a spike in reject rate was seen across product types, and root cause investigation showed that new inspectors were being trained on that day. The analysis showed an opportunity in standard clarification. In the example of the vial washing process, a periodic spike in particle reject rate was seen, and root cause investigation showed that all the rejects were from one single product. This particular product uses a different vial specification than others and required washing by a different washer. It showed an opportunity in changing the vial type or in qualifying the standard washer to be used on the new vial type to reduce the reject rate.

2.3.2 Project Introduction

2.3.2.1 Motivation

Currently, process monitoring is done separately by product. In clinical manufacturing, where multiple products are run and often in limited number of product lots, this approach takes time and does not provide comparisons from one product to another for the purpose of early process development feedback across product teams.

2.3.2.2 Project Approach

This study utilized inspection data as an initial focus for cross-product review. Statistical analysis tools were used to categorize inspection reject rates by types of containers and rejects and to set upper control limits for each. Data across

products were collected from clinical manufacturing and trended against the limits. The trends were measured, and root cause analysis was then performed for products that showed signs of violations.

2.3.3 Background Information

Because manufacturing is a dynamic process, reject rates can be expected to vary over time. The acceptable rate limits must be updated at regular intervals.

Inspection Procedures require that reject rates for vials and syringes must be evaluated regularly. The analysis helps determine if reject rates have changed over the two years and thus must be updated accordingly.

There are opportunities to review cross-product data. Regular analysis of process performance data from clinical settings can illustrate improvement opportunities and highlight risks. It can drive learning across product teams, catches weak signals that are not at non-compliance limits, and provide data-driven culture for continuous improvement.

2.3.4 Materials and Methods

2.3.4.1 Data Collection

A reject rate was calculated for each available category for each clinical syringe and vial lot produced in clinical manufacturing. The reject rate for each category was calculated by dividing the quantity of rejects in each category by the quantity of units inspected and multiplying the result by 100 to express it as a percentage. The reject rates were then documented on the clinical monitoring plan for each batch. An electronic copy of the document is stored in the database. The

data verifier looked up information of each batch for inspected quantity, reject quantity, and percentage inspection reject rate for verification. The verified data were submitted to Process Development and Quality Engineering for analysis.

2.3.4.2 Data Analysis

The statistical analyses were performed for calculating the reject rate limits for inspected drug product batches in glass vials and glass syringes in clinical manufacturing between 1/1/2013 and 12/1/2014.

Reject rate data have a non-normal distribution and thus must be transformed before reject limits can be established. In 1949, Johnson developed a flexible system of distributions, based on three families of transformations (exponential, logistic, and hyperbolic sine) that translate a non-normal variate to one that conforms to the standard normal distribution. These transformations are used to generate log-normal (SL), unbounded (SU), and bounded (SB) distributions, respectively. The coefficients defining a Johnson distribution consist of two shapes (γ, δ), a location (ξ), and a scale (λ) parameter, allowing a unique distribution to be derived for datasets with any mean, standard deviation, skewness, and kurtosis. (Montgomery, 2013). The calculation for Johnson transformation is shown below.

Equation 10: Johnson Sb Transformation

$$Z = \gamma + \delta \ln\left(\frac{x-\theta}{\sigma+\theta-x}\right)$$

where

- Z: standard normal variable
- X: reject rate (fraction)

- θ: location parameter
- γ and δ: shape parameters
- σ: reject rate

The data were analyzed and transformed for normalization using the statistical software JMP version 11. Diagnostic plots of transformed data were created to show that the transformed data are normalized (shown by having the data lie along the middle line and most of the points within the limits on the diagnostic plots). For the overall inspection and other (piston/plunger) reject rates, Johnson Sb transformation was shown to be appropriate for normalization, while the particle and component reject rates were transformed exponentially. There were not enough unique reject rates (>5 unique numbers) to set appropriate control limits for the Air gap, Volume and Solution defect subcategories, and thus these subgroups were not part of the scope.

After data have been transformed, control limits for each defect subcategory was set. The one-sided upper control limit (UCL) was set using quantile at 99.865% (three sigma value). JMP automatically calculates the limits with the data inputs using the following equations.

Equation 11: Upper Tolerance Limit Calculation

Upper Tolerance Limit (UTL) $= \bar{Z} + k\,S$

Where

- $\bar{Z}$: mean of the standard normal variable (it is usually zero)
- k : one-sided tolerance multiplier

- S: standard deviation estimate of the standard normal variable.

Calculated UTL can be transformed to linear scale by solving Equation 10 for X as in Equation 12 in order to obtain the reject limit.

Equation 12: Reject Limit Calculation

$$\text{Reject Limit (\%)} = \frac{(\sigma+\theta)e^{\left(\frac{Z-\gamma}{\delta}\right)}}{1+e^{\left(\frac{Z-\gamma}{\delta}\right)}} \times 100$$

where nomenclatures are as in Equation 10.

2.3.4.3 Signals Detection

Nelson rules are a method in process control for determining if a measured variable is unpredictably out of control. The Nelson rules were first published in the 1984 by Lloyd S Nelson and have been considered a standard for control charts (Montgomery, 2013).

Figure 28 summarizes the Nelson violations commonly used. Nelson violation 1, which shows 1 point more than 3 standard deviations higher or lower than the mean, indicates that a sample is grossly out of control. Nelson violation 2, which shows at least 9 points in a row on the same side of the mean, indicates the existence of prolonged bias. Nelson violation 3, which shows at least 6 points in either increasing or decreasing direction, indicates the existence of a trend. Lastly, Nelson violation 4, which shows at least 14 points in a row in alternating increasing and decreasing directions, indicates oscillation beyond noise.

Figure 28: Nelson Violations

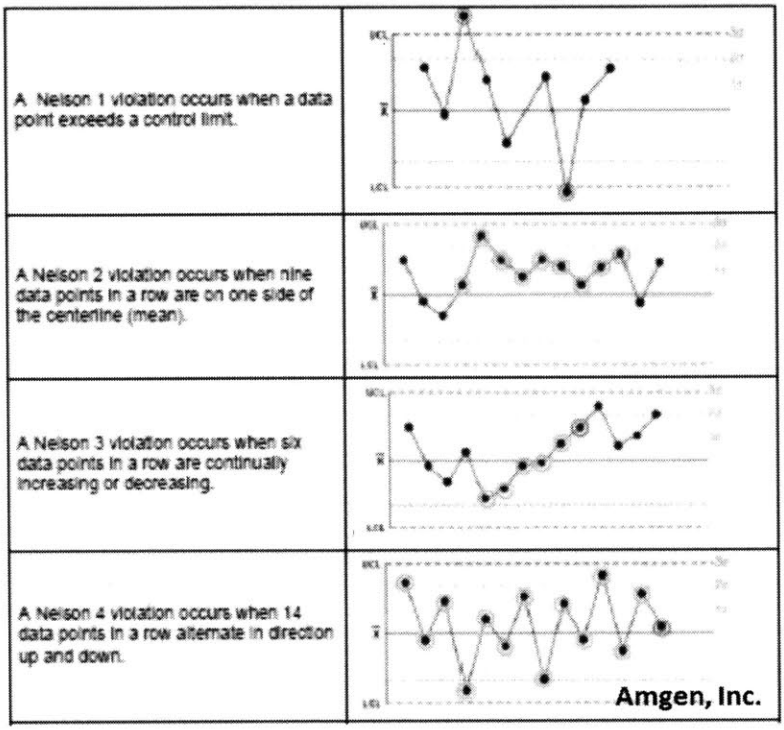

The inspection data were trended to look for Nelson violations and weak signals that could eventually lead to an out-of-control process.

2.3.4.4 Root Cause Analysis and Communication to the Stakeholders

During the monthly review of cross-product process monitoring, resources from process development, manufacturing, and quality assurance met to look at data trends. As Nelson violations or weak signals were observed, root cause analysis began by identifying problems and assigning the analysis to an appropriate resource. As the resource provided more information, a summary email of data trends and analysis was sent to key stakeholders and clinical site leadership team. Figure 29 shows the picture of the root cause analysis exercise at the clinical manufacturing site.

Figure 29: Root Cause Analysis Exercise

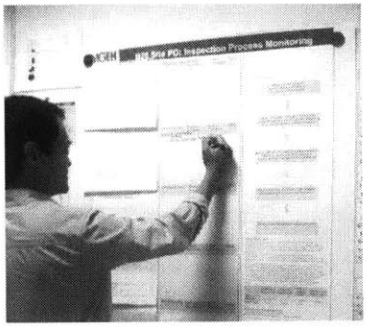

2.3.4.5 Continuous Improvement

Cross-product process monitoring initiative continuously improved based on feedback from stakeholders involved. The improvements include the following:

1. The incorporation of Electronic Batch Record (EBR) to speed up process of data collection and analysis: At the beginning of the initiative, the data collection was done manually by technicians who performed the inspection. This process was labor-intensive and error-phone. The initiative switched to using the data from the EBR, a required data logging system for clinical manufacturing. The switch eliminated the separate data collection and sped up the data analysis process.
2. The change to electronic review process as the plant meetings become electronic: Initially the data trends were printed and reviewed monthly on a board as shown in Figure 29 above. As the plant meetings moved from on-the-floor reviews to conference room setting, the initiative moved with it, changing the format to the electronic reviews.

3. Training for sustainment: To ensure that the initiative would be carried forward, a resource from process development was trained as the lead.

Figure 30 summarizes the approach that the cross-product process monitoring initiative took and the improvements it implemented based on feedbacks from the stakeholders.

Figure 30: Approach to Process Monitoring Initiative and Improvements

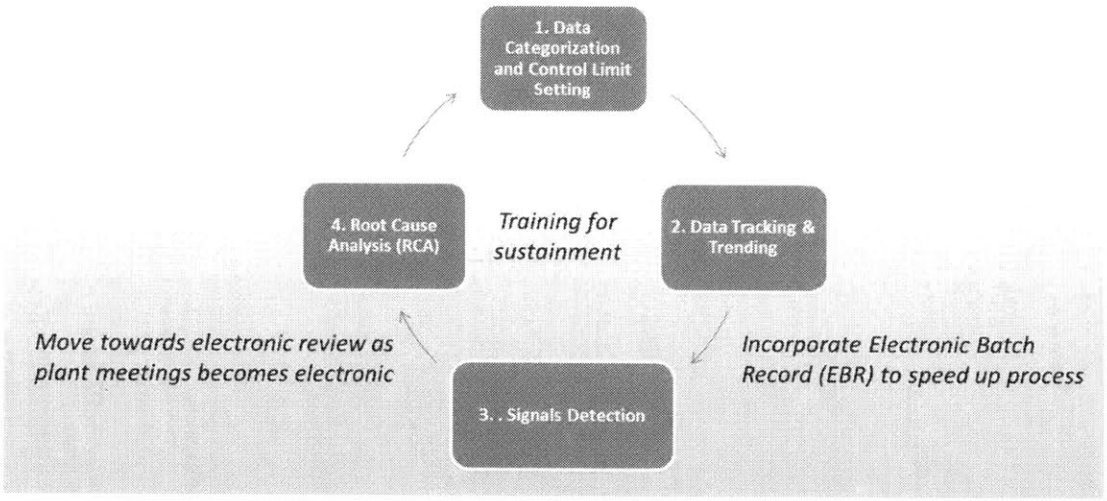

2.3.5 Results and Discussion

2.3.5.1 Data Analysis

Data analysis was conducted on final products' defect rates. High-level results are shown through statistical transformation in Figures 31 and 32.

Figure 31: Syringe Inspection Reject Rate Histogram, Johnson Sb Transformation, Quantile Limits, and Run Chart (April 2013-Dec 2014)

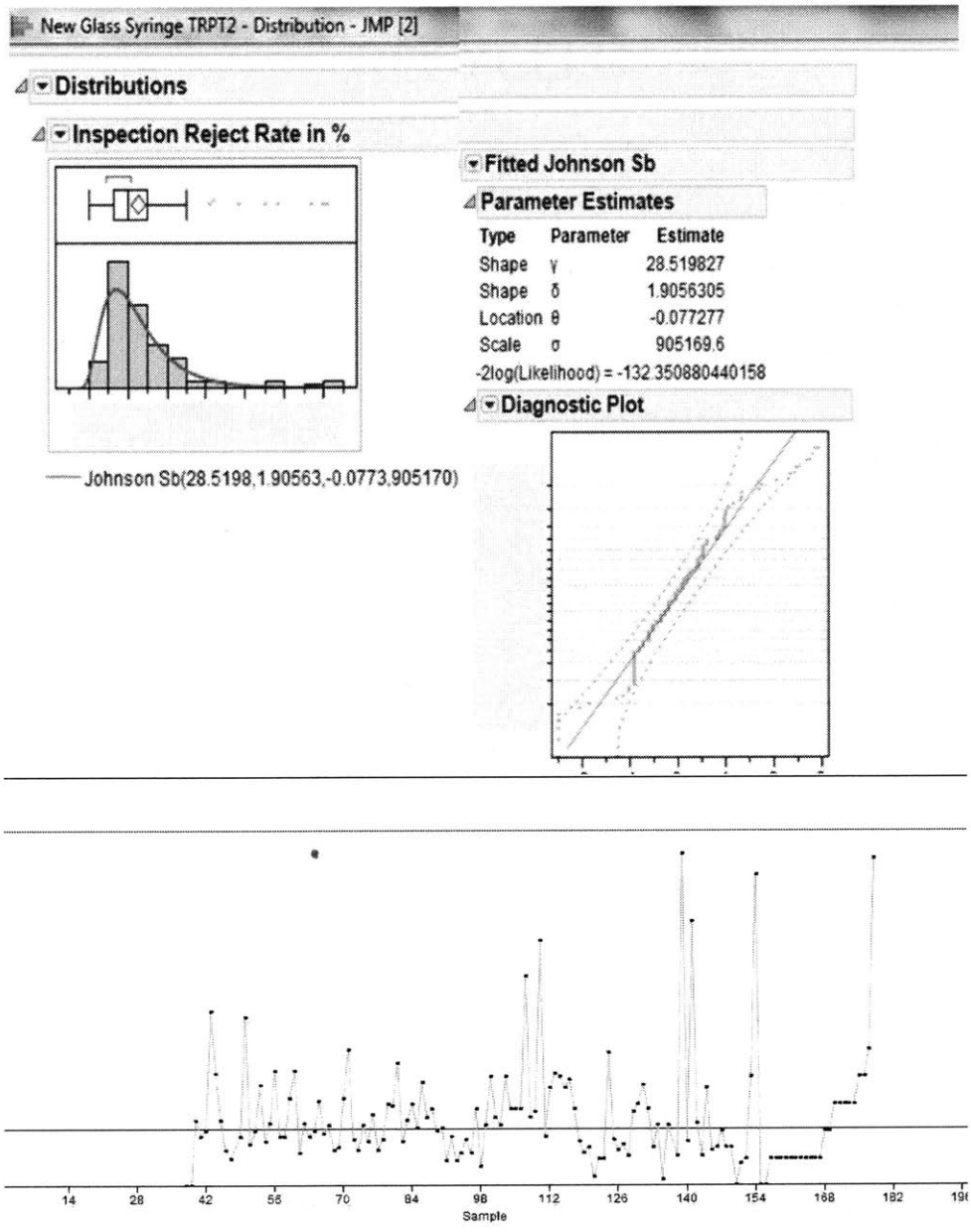

The particle, other (piston/plunger), and component reject rates were analyzed in the same fashion.

Figure 32: Vial Overall Inspection Reject Rate Histogram, Johnson Sb Transformation, Quantile Limits, and Run Chart

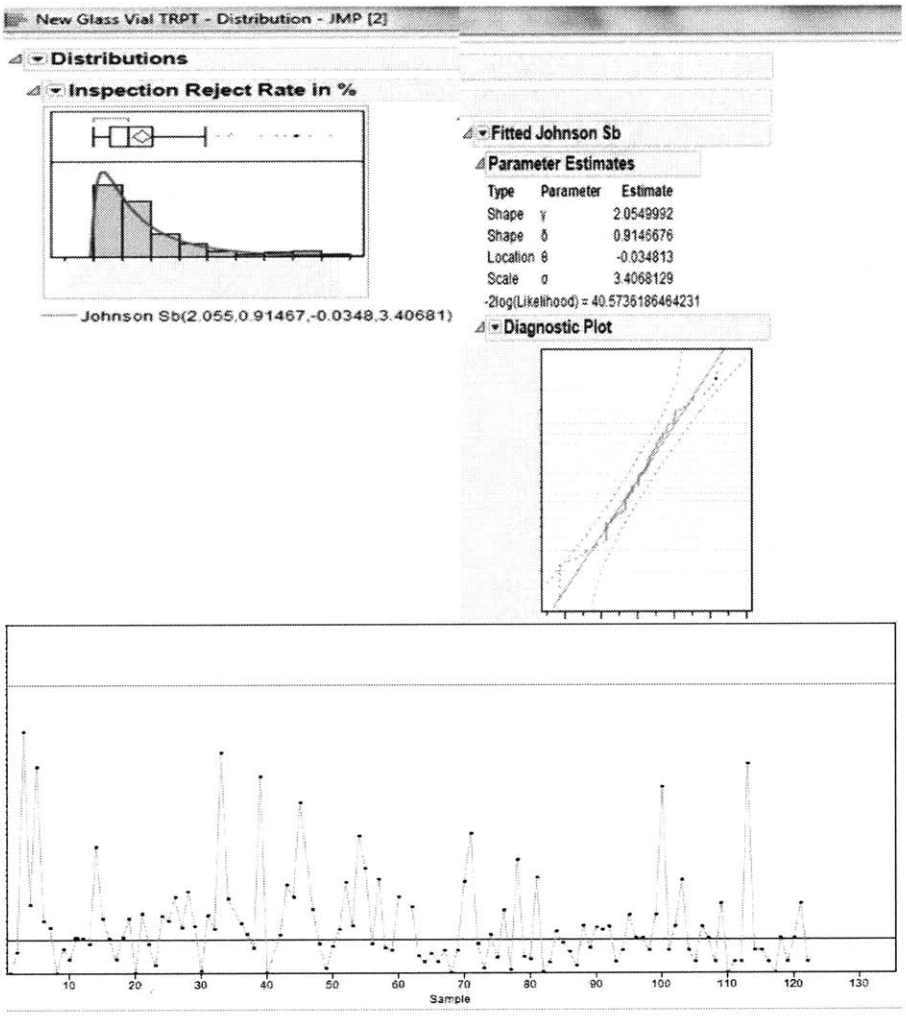

The particle, other (piston/plunger), and component reject rates were analyzed in the same fashion.

2.3.5.2 Examples of Root Cause Analysis

Regular analysis of process performance data from clinical settings can illustrate improvement opportunities and highlight risks. Two examples are shown below.

2.3.5.2.1 **Improvement in Training**

The trending of inspection data showed an elevated data point which alerted us to evaluate a cause and determine any action needed. (Figure 33). Root cause analysis indicated that the product inspection was performed by new temporary inspection staff, revealing opportunities to improve the standards for training.

Figure 33: Trend Showing Potential Improvement in Training

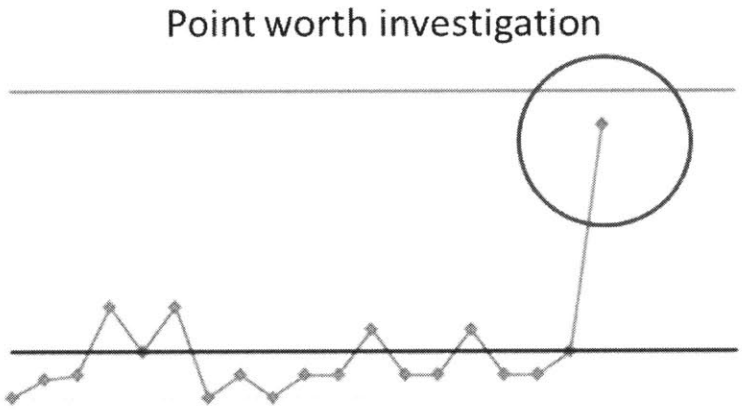

2.3.5.2.2 **Improvement in Process**

The trending of particle reject rates showed that particle rejects did not happen frequently. However, six lots of products showed particle rejects in the same period of time (Figure 34).

Figure 34: Trend Showing Potential Improvement in Process

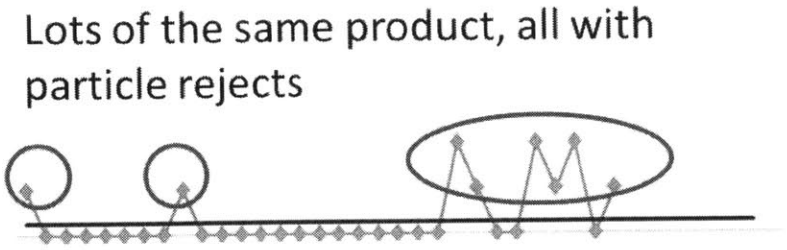

Root cause analysis showed that all the lots were of the same product. This product is processed on unique equipment based on its configuration. This was identified as a potential contributing factor and may lend opportunity to modify the equipment or operation.

2.3.6 Conclusion and Recommendations

The cross-product process monitoring of inspection rates in clinical manufacturing showed improvement opportunities and highlighted risks. The insights generated for the last three months have increased the stakeholders' buy-in, generating business case for the needs of this effort. Additionally, systems that the clinical manufacturing used, including electronic batch record and work center team meeting format, have been integrated. Lastly, a resource from process development has been trained to carry the initiative forward. To take the initiative further, advanced opportunities, as identified by key parameters for other unit operations, should be carried out. The necessary plans in place to ensure the sustainment of this initiative are highlighted in Figure 35.

Figure 35: Plans for Ensuring the Sustainment of Cross-Product Process Monitoring

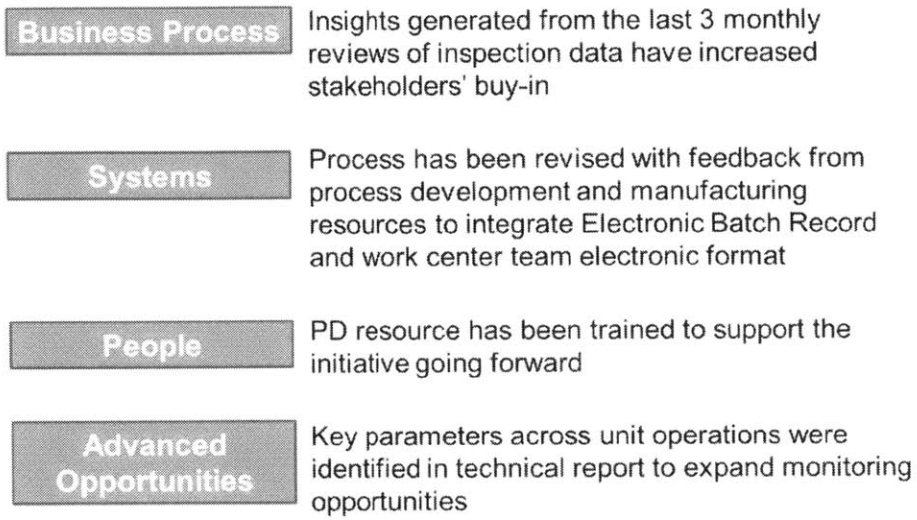

3 Conclusion

Through the aforementioned case studies, new approaches to process design were proposed for the Drug Product Technology group within the Drug Product Commercialization and Manufacturing Network. The proposed strategy suggested broad objectives for process improvement at each step based upon and increased understanding of the fundamentals of each unit operation. Three specific project case studies within the project landscape were explored in the body of this thesis. For each case study, the needs, benefits, potential pitfalls, and recommendations moving forward were discussed.

A proof-of-concept model for drug product drying at the filling nozzle was developed to illustrate the benefits of First Principles modeling. Additionally, a CFD model for the filling nozzle was used to help visualize the dripping phenomenon experienced during the filling process. These two case studies illustrate that First Principles can be used to improve process understanding and robustness in drug product unit operations. Key criteria for evaluating cost/benefit of topics to be modeled with First Principles were generated to help guide future studies.

Another approach to process design is through learning from products that have completed technology transfer to clinical manufacturing. The cross-product process monitoring initiative illustrates how process performance data analysis can be used to catch weak signals and highlight operational improvement opportunities. A business process for inspection data reviews was established and deployed with

involvements from process development, manufacturing and quality assurance groups to enable cross-functional engagement and to share learning.

4 References

Amgen, Inc. (2014, February 17). *Pipeline*. Retrieved January 15, 2015, from http://www.amgen.com/science/pipe.html.

Amgen, Inc. (2015, January 5). *About Amgen Fact Sheet*. Retrieved January 15, 2015, from http://www.amgen.com/pdfs/misc/Fact_Sheet_Amgen.pdf.

Beverung, C.J., Radke, C.J., and Blanch, H.W.(1999) *Protein Adsorption at the Oil/Water Interface: Characterization of Adsorption Kinetics by Dynamic Interfacial Tension Measurements*. Biophys Chem. *1999* Sep 13;81(1):59-80.

First Ten Angstroms. (2000) *A Simple Introduction to the LaPlace Equation*. Accessed October 10, 2014. http://www.firsttenangstroms.com/pdfdocs/SimpleLaplaceEquation.pdf.

IBISWorld (2015, January). *Global Biotechnology Market Research Report*. Retrieved on February 16, 2015, from http://www.ibisworld.com/industry/global/global-biotechnology.html?partnerid=prweb.

JP Morgan. (2015, January). 2015 Global Biotech Outlook. Retrieved on February 16, 2015, from https://www.jpmorgan.com/cm/BlobServer/2015-healthcare-01.pdf?blobkey=id&blobwhere=1320662161195&blobheader=application/pdf&blobheadername1=Cache-Control&blobheadervalue1=private&blobcol=urldata&blobtable=MungoBlobs.

Lambert, P. (2008). *Dispensing Biopharmaceuticals with Piston and Peristaltic Pumps. Pharmaceutical Technology. Equipment and Processing Report*, 17 September. Iselin, NJ: Advanstar Communications.

Meyer, B. K., & Coless, L. (2012). *Compounding and Filling: Drug Substance to Drug Product.* Therapeutic Protein Drug Products: Practical Approaches to formulation in the Laboratory, Manufacturing, and the Clinic, 83.

Montgomery, D. *Introduction to Statistical Quality Control*, 7th Ed., Wiley, 2012, p 204.

Pordal, HS, CJ Matice, and TJ. Fry. (2002). *The Role of Computational Fluid Dynamics in the Pharmaceutical Industry*. Pharmaceut. Technol. N. Am. Feb.

Shieu, W, S Torhan, E Chan, et al. *Filling of High-Concentration Monoclonal Antibody Formulations into Pre-Filled Syringes: Filling Parameter Investigation and Optimization.* PDA J Pharm Sci Technol. 2014 Mar-Apr; 68(2):153-63.

Tripp, B.C., Magda, J.J., and Andrade, J.D (1995). *Adsorption of Globular Proteins at the Air/Water Interface as Measured via Dynamic Surface Tension: Concentration*

Dependence, Mass-Transfer Considerations, and Adsorption Kinetics. J. Colloid Interface Sci. *1995*, 173, 16-27.

Wilkes, James O., *Fluid Mechanics for Chemical Engineers with Microfluidics and CFD*, 2nd Ed., Prentice Hall, 2005.

Woodward , R. P. *Surface Tension Measurements Using the Drop Shape Method*. Accessed October 10, 2014. http://www.firsttenangstroms.com/pdfdocs/STPaper.pdf.